SEDIMENTATION OF THE BRAZOS RIVER SYSTEM: STORAGE IN THE LOWER RIVER, TRANSPORT TO THE SHELF AND THE EVOLUTION OF A MODERN SUBAQUEOUS DELTA

A Dissertation

by

JOSEPH ANDREW CARLIN

Submitted to the Office of Graduate Studies of
Texas A&M University
in partial fulfillment of the requirements for the degree of

DOCTOR OF PHILOSOPHY

Chair of Committee,	Timothy Dellapenna
Committee Members,	William Bryant
	Chris Houser
	William Sager
Head of Department,	Piers Chapman

August 2013

Major Subject: Oceanography

ABSTRACT

The Brazos River, located predominantly within the state of Texas, has the highest water and sediment discharge of all rivers in the state, and ranks second behind the Mississippi River in terms of sediment load delivered to the Gulf of Mexico. This river is the only Texas river that consistently drains directly into the Gulf of Mexico forming a wave-dominated delta. The delta has experienced dramatic and rapid changes over the last 100-plus years. These changes have resulted from both natural and anthropogenic alterations to the coastal zone proximal to the river mouth and within the rivers watershed. By utilizing high-resolution geophysical data, sediment cores, water column data, and historic shoreline data this study investigated the mechanisms in which sediment is transported to the coastal ocean, the fate of that sediment as it becomes preserved in the modern geological record, and the evolution of a modern delta.

Results from this study show that during for a majority of the time a salt-water intrusion in the lower river traps sediment, preventing export to the coastal ocean. The trapped sediment forms an ephemeral mud layer in the lower river that may be remobilized during increased river discharges. When river discharges increase above an observed threshold of 300 m^3/s the salt wedge is pushed seaward of the river mouth and sediment is exported via a buoyant plume. As export of sediment is episodic, accumulation of sediment on the subaqueous delta characterized as non steady-state, and resembles typical foreset delta attributes. These include

physical stratification of sediment layers, episodic but relatively high rates of accumulation, and little bioturbation. Currently sediment is primarily accumulating west of the river mouth, and the majority of sediment is bypassing the system. Over the history of the delta, changes both anthropogenic and natural have shifted the relative balance of fluvial sediment supply and marine sediment dispersal. These changes have resulted in dramatic changes in the shoreline, and phases of activation and abandonment of deltaic lobes, which can be seen through historical data and imagery, and is preserved in the recent sedimentary record.

DEDICATION

I dedicate this work to my wife Mary, and my daughter Mabel for their endless love and support.

ACKNOWLEDGEMENTS

I would like to thank my committee chair, Dr. Tim Dellapenna, and my committee members, Dr. Bill Bryant, Dr. Chris Houser, and Dr. Will Sager, and for their guidance and support throughout the course of this project.

I would also like to thank the members of the Coastal Geology Lab, past and present, for all their assistance along the way. In addition I would like to thank the faculty and staff of the Department of Oceanography in College Station, and the Department of Marine Science in Galveston. Thanks also go to the staff of the Research and Graduate Studies Office in Galveston for all of their help. Finally, I would like to thank the Texas General Land Office for funding the offshore surveys and core collection, and the crew of the R/V Manta.

NOMENCLATURE

CTD	Conductivity Temperature and Depth Instrument
OBS	Optical Backscatter Sensor
SSC	Suspended Sediment Concentration
SSS	Side Scan Sonar
USGS	United States Geological Survey
MLW	Mean Low Water
ICWW	Intracoastal Water Way
SH36	State Highway 36
GOM	Gulf of Mexico
OBD	Old Brazos Delta
MBD	Modern Brazos Delta
IODP	Integrated Ocean Drilling Program
PBRMF	Proximal Brazos River Facies
DBRPF	Distal Brazos River Plume Facies
GOIMF	Gulf of Mexico Innershelf Facies
BDBR	Brazos Delta Beach Ridges

TABLE OF CONTENTS

LIST OF FIGURES

Page

1 INTRODUCTION

River mouths are the most fundamental element of a deltaic system as they are the dispersal point for terrestrial sediments to the marine environment (Wright, 1977). Upon entering the ocean, marine processes can subject riverine sediment to alteration via periods of deposition, resuspension, and secondary transport prior to preservation in the stratigraphic record (Wright and Nittrouer, 1995). This establishes a distinction between sediment deposition, a relatively short-term process, and the long-term sediment accumulation. With an estimated annual flux of 20 billion tons of fluvial sediment reaching the worlds oceans (Milliman and Syvitski, 1992), understanding the fate of fluvial sediment in the marine environment, both in terms of deposition and accumulation, is important for a variety of processes that link terrestrial and oceanic systems including organic carbon cycling (Bianchi and Allison, 2009), and the creation of the geologic record (Nittrouer et al., 1996).

The focus of this dissertation is to understand the mechanisms that influence the flux of sediment from the Brazos River to the Gulf of Mexico, the sedimentation on the proximal shelf/subaqueous delta that results, and how changes in sedimentation over the modern history of the delta have contributed to the evolution of the system. This dissertation is organized in sections, where each section is prepared as a stand-alone manuscript for publication in a scientific journal, but each section also builds on the previous section(s) to create a comprehensive picture of Brazos River sedimentation in the coastal ocean.

The first section focuses on the lower ~ 15 km of the river, and the proximal shelf seaward of the mouth. This section investigates the influence of a marine water intrusion (salt wedge) on the fluvial suspended sediment, and the implications for sediment export to the Gulf of Mexico. By comparing data from CTD sampling, supplemented with sediment core and geophysical data, to river gage measurements the frequency of sediment export events from the river to the Gulf of Mexico was estimated.

The second section focuses on the sediment on the subaqueous delta to better understand the fate of the fluvial sediments in the coastal ocean. Primarily through sedimentological techniques, this section distinguishes Brazos River sediment from Gulf of Mexico shelf sediments, describes and quantifies sediment accumulation within the study area on the subaqueous delta, and determines changes in sedimentations over time. This section also estimates a sediment budget for the study area, determining the fraction of the annual sediment load of the river that is preserved in the sediments proximal to the mouth.

Finally, the third section utilizes historic imagery and data, compared to data collected during this study to investigate the evolution of the delta. This third section focuses on how changes in the relative balance between fluvial sediment supply and marine sediment dispersal over time have resulted in feedbacks in the system as the delta shifts toward the maintenance of a dynamic equilibrium. The evolution of the delta, observed

in the changes to the shoreline of the subaerial delta and preserved in the sedimentary record of the subaqueous delta, is driven by natural and anthropogenic alterations to the river, the watershed, and to coastal zone that affect either the sediment supply, sediment preservation on the shelf, or both.

2 THE INFLUENCE OF A SALT WEDGE INTRUSION ON FLUVIAL SUSPENDED SEDIMENT AND THE IMPLICATIONS FOR SEDIMENT TRANSPORT TO THE ADJACENT COASTAL OCEAN

2.1 Introduction

River mouths are the most fundamental element of a deltaic system as they are the dispersal point for terrestrial sediments to the marine environment (Wright, 1977). Globally, 10-20 billion metric tons of sediment are transported by rivers to the oceans each year (Milliman and Syvitski, 1992), additionally rivers also transport terrestrial organic carbon to the ocean, which can influence global biogeochemical cycles and ocean sequestration of carbon dioxide (Bianchi and Allison, 2009). Understanding the conditions at the river mouth that may facilitate or impede transport of sediment is important in understanding the flux of terrestrial material to the ocean.

Sediment discharge from a river is primarily related to basin size, topography, precipitation, and sediment erodability (Milliman and Syvitski, 1992). Although most of these factors respond to changes within the watershed, it is those factors influencing the sediment discharge at the river mouth that may be most important in determining, and predicting the fate of terrestrial material entering the ocean (Syvitski and Morehead, 1999). At the river mouth, when marine processes (tides and waves) are negligible or small compared to river outflow, one or more of three process will dominate: inertia, turbulent bed friction, or buoyancy; and when buoyancy dominates, where the river mouth is deep relative to river discharge a salt wedge can intrude into the river (Wright,

1977). Studies have shown the movement of a salt wedge within a river is largely influenced by river discharge (Geyer et al., 2001; Islam et al., 2002; Kineke et al., 1996) as the momentum of the fresh water outflow from the river interacts with the force of the intruding marine waters (Geyer et al., 2004). Principally, theses studies have shown seaward movement of the salt wedge during periods of increased fresh water discharge to illustrate a mechanism for sediment transport out of a river or estuary to the coastal ocean. For example, during the times of high discharge on the Amazon River, the salt front can be displaced from the river over 100 km from the mouth, both across the shelf as well as hundreds of kilometers along the shelf (Geyer and Kineke, 1995; Gibbs, 1970; Nittrouer et al., 1986a). During high discharge on the Mississippi river, the salt wedge may also be located seaward of the river mouth, but during low discharges, the salt wedge may migrate landward to the lower reaches of distributary channels (Wright, 1971).

Common to estuaries, sediment can be trapped at the salt wedge, forming an estuarine turbidity maximum due to a variety of factors. These include: the convergence of landward and seaward flows, resuspension by tidal currents which transports sediment both landward and seaward to a singular null point (Dyer, 1994; Postma, 1967), flocculation due to the interaction of sediment particles with the salt water that increases the settling velocity enhancing the downward flux (Kineke et al., 1996), and reduced turbulence due to salt stratification that reduces the amount of sediment that can be carried by the flow (Geyer, 1993). Where a salt wedge is typically present in the lower

reaches defines the estuarine zone of the river, where estuary-like conditions persist (Galler and Allison, 2008). This suggests that within this zone the sediment distributions and river bed features would approximate a typical estuary, with a fluvial and marine end member separated by a muddy middle reach where the salt wedge traps fine grained sediments (Dalrymple et al., 1992). Galler and Allison (2008) observed such conditions in the lower Mississippi River as a salt wedge trapped sediment during lower discharges, forming an ephemeral mud layer, a few meters in thickness, that was remobilized and exported during increased discharge when the salt wedge, and estuarine zone were relocated seaward of the river mouth. A salinity intrusion has been also observed in the Brazos River (Keeney-Kennicutt and Presley, 1986), which like the Mississippi also empties in to the Gulf of Mexico. However, to date no study has focused on the impact of the salt wedge on sedimentation, specifically suspended sediment, and sediment export to the Gulf of Mexico.

This study investigates the lower reach of the Brazos River, to determine how the salt wedge and estuarine conditions affect suspended sediment, primarily how these conditions influence the timing of sediment export to the coastal ocean. Utilizing Conductivity, Temperature and Depth (CTD) data coupled with Optical Backscatter Sensors (OBS) the location and extent of the salinity intrusion and Suspended Sediment Concentrations (SSC) were determined for different fluvial discharge levels. In addition, high-resolution Side Scan Sonar (SSS) coupled with swath bathymetry and sub-bottom sonar data were used to investigate sediment distributions, and bed elevation changes

over different fluvial discharge conditions. The goals of this study are (1) to distinguish the estuarine zone of the lower river, (2) to investigate the interaction of the salt wedge on suspended sediment, (3) define the conditions that determine when the salt wedge is present in the lower river, and when the fresh water-sea water convergence zone is seaward of the river mouth, (4) develop a conceptual model that describes the timing and nature of sediment export from the river to the Gulf of Mexico, and (5) and discuss the implications for how this can influence estimates for the annual flux of sediments to the global ocean.

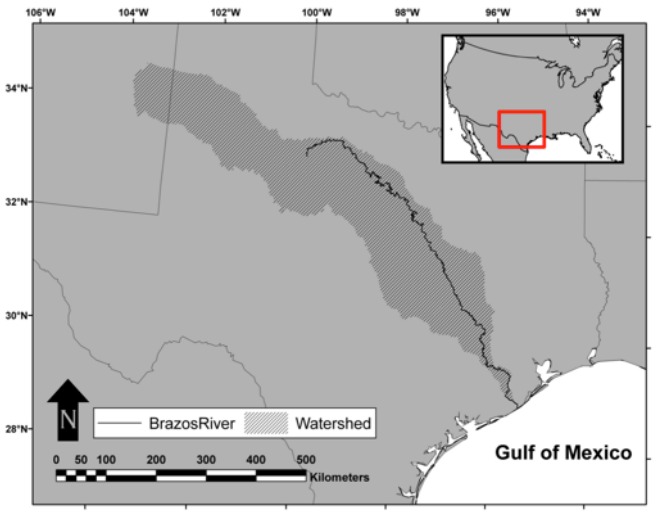

Figure 1: Map of Brazos River (black line) with watershed (shaded area).

2.2 Background

The greatest amount of contiguous United States sediment is transported to the Gulf of Mexico, where the Brazos River is second only to the Mississippi River in terms of tons of sediment delivered to the Gulf of Mexico (Milliman and Meade, 1983), which is

estimated at ~ 10 - 16 Mt/yr. The Brazos River is the 11th longest river in the United States with an 118,000 km^2 watershed encompassing areas in northeastern New Mexico and large portions of Texas (Figure 1). It has the highest rate of flow and sediment yield of all Texas rivers (Rodriguez et al., 2000), and is the only river on the Texas coast that consistently drains into the Gulf of Mexico. The mean annual discharge of the river is 214 m^3/s since 1940 (Dunn and Raines, 2001; Sylvia and Galloway, 2006), over half of all precipitation in the watershed falls below the lowermost main stem reservoir, and the lower 40 kilometers of the river is heavily modified by channelization and levees preventing direct connection to the floodplain (Texas Water Development Board). Therefore overbank flooding is minimal, and most of the fluvial sediment is stored in the lower river and not within the flood plain. Arguably the most significant modification to the system occurred in 1929 when the United States Army Corps of Engineers moved the river mouth ~ 10 km to the southwest. This study area encompasses the entire diverted section of the lower river (~ 10 river kilometers), and a section immediately above the diversion (~ 5 river kilometers).

Figure 2 shows the rating curve from the river calculated from data from the Richmond gaging stations for the years between 1966 and 1986. The curve shows there is a strong positive relationship between the fluvial discharge and the suspended sediment concentration (SSC) within the river (Syvitski et al., 2000). The Richmond gage station is located approximately 150-river km upstream from the mouth.

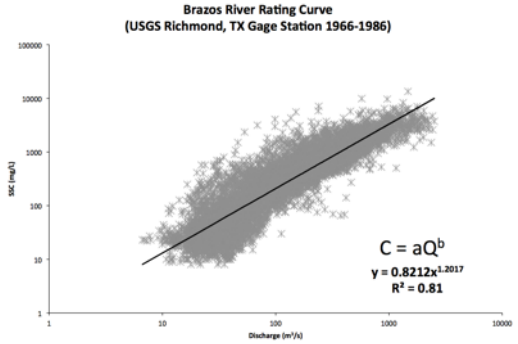

Figure 2: Rating curve for the Brazos River based on data from the US Geological Survey (USGS) river gage station at Richmond, TX. Measurements consist of average daily discharge (m^3/s) and daily suspended sediment concentration (mg/L) for years 1966 to 1986. Rating curve equation shown, where C is concentration, Q is discharge and a and b are coefficients.

2.3 Methods

2.3.1 Sampling Effort

In 2007 two cruises were conducted during and following a significant flood event. This event reached a peak average daily discharge in excess of 2000 m^3/s, a 4-year recurrence interval since 1960, however in terms of duration at elevated discharges, this represents a 25 year flood. These cruises focused primarily on collecting water column data with stations located along a transect extending from offshore to inside the river (Figure 3b). In the summer of 2010, three additional cruises took place during various river discharges. Sampling stations were located every 0.5 km extending 15 km upriver from the river mouth (Figure 3a). In January 2012 a cruise collected data from both in the river and on the shelf. This cruise re-occupied the same 2010 river sampling stations, and 29 stations on the shelf distributed over approximately a 65 km^2 area centered around the river mouth (Figure 3c).

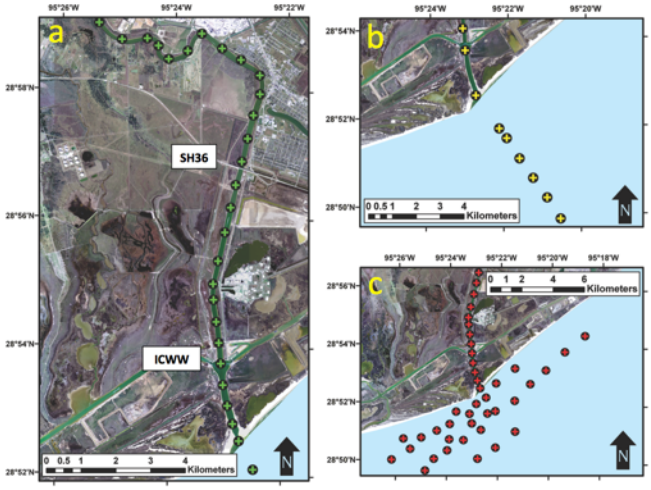

Figure 3: Maps of sampling stations during: (a) 2010 cruises (b) 2007 cruises; and (c) January 2012 cruise. Panel (a) identifies locations for Intracoastal Waterway (ICWW) and State Highway 36 (SH36) bridge crossings.

2.3.2 Water Column Sampling

A Sea-bird Electronics SeaCAT Profiler CTD *SBE* 19plus with a Seapoint Turbidity Meter was deployed for most cruises at all stations to measure conductivity, temperature, depth and optical backscatter. For the January 2012 sampling cruise an RBR XR-420 CTD with Seapoint Turbidity meter was used. OBS data were converted to SSC using calibration curves developed in the laboratory using mud samples collected from the riverbed to approximate fluvial suspended sediment. River discharge data were acquired from the USGS river gage station 08116650 at Rosharon, TX approximately 100-river km from the mouth. No major tributaries enter the Brazos River between the Rosharon gage station and the mouth.

2.3.3 Geophysical Surveys

SSS, swath bathymetric and sub-bottom data were collected on various cruises within the lower river. Swath bathymetry and SSS were collected in 2010 during the May and June cruises using a 200 kHz Teledyne Benthos C3D-LPM High-Resolution Side-Scan Sonar and Swath Bathymetric System that collects swath bathymetry and SSS data concurrently. Bathymetric data were corrected to Mean Low Water (MLW) using NOAA tide station 8772447 located at the US Coast Guard station in Freeport, TX located approximately 10 km from the river. Sub-bottom data were collected during an August 2011 cruise using an Edgetech 216 Full Spectrum Sub-bottom CHIRP seismic sonar operating on frequencies between 2 and 16 kHz.

2.3.4 Sediment Analysis

Surface sediment samples were collected during the May 2010 cruise. Sediments samples were analyzed in the lab for grain size distributions using a Malvern Mastersizer 2000® laser particle diffractometer. Sediment samples were homogenized, combined with a dispersant and sonicated to prevent and break up flocs prior to measurement. The instrument determined percent composition of sand, silt and clay of the samples, as well as mean grain size and other statistical parameters.

2.4 Results

2.4.1 Water Column Data

Results from the July 12, 2007 are shown in Figure 4a. Sampling occurred near the peak of the flood in 2007 with a river discharge of approximately 1800 m^3/s (Figure 4c). Unfortunately no credible salinity data are available for this date due to a miscalibrated sensor, but SSC concentrations were collected along a transect extending offshore from the river mouth (Figure 3b). SSC data show a high concentration layer at the surface, extending offshore from the mouth approximately 4.5 km. The thickness of this surface plume is about 2 m, with highest concentrations just below 500 mg/l. In addition to the surface plume, elevated SSC concentrations were also observed in the bottom waters, where concentration range between 100-200 mg/l for most of the area extending almost 5.5 km from the river mouth. This bottom boundary layer is thickest in the nearshore region of the transect (~ 3 m), and thins offshore (< 1m).

Following the July 2007 event, a sampling cruise was conducted on October 13, 2007 (Figure 4b) during the falling limb of the Summer 2007 flood. At this time the river discharge had returned to near mean discharge, ~260 m^3/s (Figure 4c), and samples were collect along the same transect as the July cruise, but also included three stations in the river. Salinity data (white dashed contours Figure 4b) show a salinity intrusion into the lower river in the form a salt wedge. The 10 PSU isohaline extends from the surface waters at the river mouth, up river for the extent of the study area (> 3 km up river). SSC concentrations are generally low, much of the area both offshore, and in the river

have concentrations <100 mg/l. The highest SSC were observed in the bottom waters proximal to the river mouth with concentrations between 100-200 mg/l. The location of this bottom turbid layer corresponds to the area with the largest horizontal salinity gradient observed.

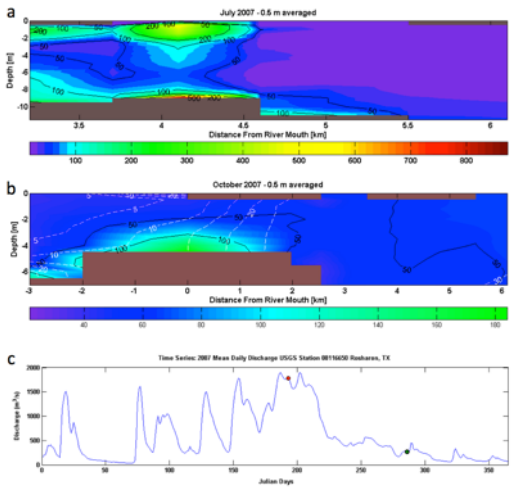

Figure 4: Water column data from 2007 sampling cruises in July (a) and October (b). Transect sampling locations shown in Figure 3. Colors and black contours show SSC in mg/l averaged over 0.5 m bins from CTD data, x-axis is distance from river mouth in km, positive values are seaward of the river mouth, negative values are up river, and y-axis is water depth in meters. Dashed white contours in (b) show salinity. No salinity data is available for July (a) due to a miscalibrated sensor. Hydrograph for the year from the USGS gage station at Rosharon, TX shown in (c) with sampling dates for July (red circle) and October (green circle).

Data from the 2010 cruises are shown in Figure 5. Starting with the May 17th cruise (Figure 5a), river discharge was comparable to the October 13, 2007 sampling with a moderate discharge of ~220 m^3/s (Figure 5d). Salinity data show a salt wedge is clearly present in the river with a steep vertical salinity gradient. The 10 PSU isohaline extends from the surface of the water at the river mouth to the riverbed approximately 6.5 km up river. This salinity pattern is similar to what was observed in October 2007, but with

increased sampling upriver during this time the full extent of the intrusion was observed. However the SSC distribution observed during this time is distinctly different from October 2007. A clear partition of SSC is observed with the majority of the suspended sediment located within the freshwater fraction of the river. Within this fresh water, concentrations were observed to be between 200- 300 mg/l, while within the saltwater concentrations were considerably lower, generally less than 100 mg/l.

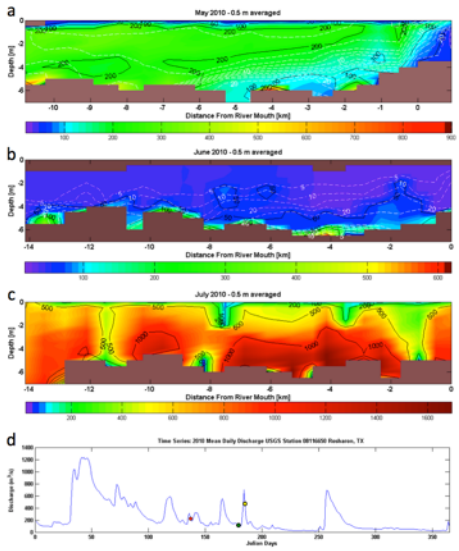

Figure 5: Water column data from 2010 sampling cruises in May (a), June (b), and July (c). Transect sampling locations shown in Figure 3. Colors and black contours show SSC in mg/l averaged over 0.5 m bins from CTD data, x-axis is distance from river mouth in km, positive values are seaward of the river mouth, negative values are up river, and y-axis is water depth in meters. Dashed white contours show salinity. No salinity was detected for July (c) indicating no salt wedge in the river. Hydrograph for the year from the USGS gage station at Rosharon, TX shown in (c) with sampling dates for May (red circle), June (green circle), and July (yellow circle).

The following month, on June 28, 2010 (Figure 5b), sampling occurred during a time of reduced discharge, ~115 m^3/s (Figure 5d). During this time the presence of salt water is evident throughout the entire study area, beyond 14 km from the river mouth. SSC is

low, 50 mg/l or less for much of the water column. SSC values increase, >100 mg/l, only within the bottom 1 m of the water column, indicating that even with a potential surface plume seaward of the river mouth, as both the 5 and 10 PSU isohalines were at depths of 1 and 2 m below the surface respectively at the mouth, sediment concentrations are negligible.

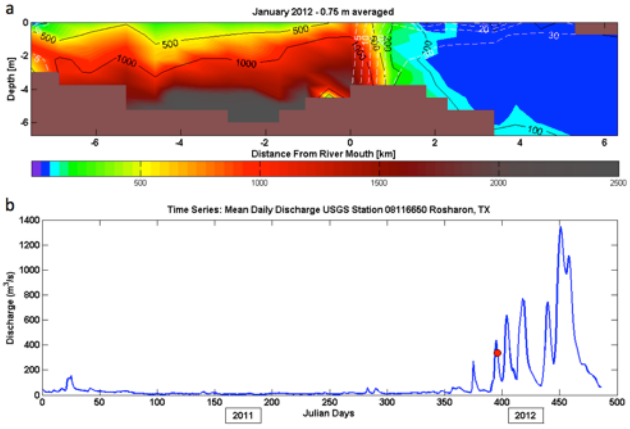

Figure 6: Water column data from January 2012 sampling cruise. (a) Sampling transect from river to offshore showing SSC colors and black contours, dashed white contours show salinity. Negative x values indicate kilometers up river from river mouth, and positive is distance offshore from river mouth. (b) 2012 hydrograph from the USGS gage station at Rosharon, TX – red circle indicates sampling date.

Figure 5c shows data collected on July 4, 2010, one week following the June 28th cruise. During this time discharge had increased, ~490 m^3/s (Figure 5d) following a peak discharge of nearly 700 m^3/s. Data showed no salinity intrusion was present within the river. The offshore conditions were too rough for offshore sampling during this event, so it was not possible to determine the extent of fresh water on the shelf. Measured SSC were high, from 500-1500 mg/l through most of the water column. The highest values

were observed in the bottom half of the water column between 2 and 8 km from the river mouth.

The last of the sampling cruises occurred on January 31, 2012 (Figure 6). Following the worst one-year drought since precipitation data have been recorded (Nielsen-Gammon, 2012), discharge had increased to ~330 m^3/s (Figure 6b). This sampling reoccupied some of the stations in river from the 2010 cruises and additional stations on the shelf (Figure 3c). The cross-section in Figure 6a shows salinity and SSC data along a transect extending from the river out on the shelf along the main axis of the buoyant plume (Figure 7a). Similar to July 2010, no salinity intrusion was observed within the river. However, directly seaward of the river mouth the water was well mixed (vertically oriented isohalines), and a large horizontal salinity gradient was observed. Further seaward of this point, a relatively thin buoyant plume is observed, generally no more than 1.5 m thick (Figure 7a). On the shelf SSC in the buoyant plume is highest directly seaward of the river mouth, observed to be >500 mg/l (Figure 7b), but within a few kilometers the concentration was reduced to less than 50 mg/l. Although SSC in the buoyant plume decreased sharply, Figure 6a does show elevated SSC (~100 mg/l) in the bottom waters offshore, similar to what was seen during the July 12, 2007 flood sampling. SSC in the river is extremely high, often in excess of 1000 mg/l. The highest concentrations were observed in the lower 1-1.5 m of the water column between River km 1 and 5. The precise concentration was difficult to determine because the concentrations exceeded the saturation limit of the OBS sensor. This saturation limit of

the sensor was empirically determined in the lab to be between 2000- 2500 mg/l. Laboratory SSC determinations from bottom waters collected from this region estimated concentrations on the order of 10^4 mg/l (or 10's of g/l).

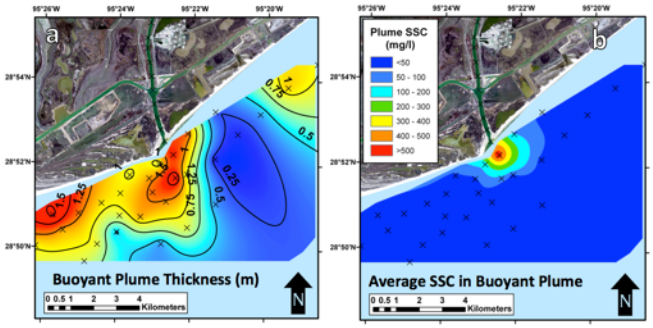

Figure 7: Plume data from the January 2012 cruise. The thickness of the buoyant plume offshore in meters (a) based on CTD data, and (b) the average SSC of the plume in mg/l. Sampling locations marked by Xs.

2.4.2 Side Scan Sonar

The side scan sonar (SSS) mosaic collected on June 28, 2010 is shown in Figure 8. In this mosaic, the lighter colors correspond to high backscatter, while dark colors represent low backscatter. Three distinct backscatter areas are observed within the study area occupying the lower, middle and upper reaches of the study area. The lower reach, from the mouth to the ICWW intersection, the SSS mosaic shows high backscatter and relatively small bedforms. In this reach the bedforms observed include shoreline or riverbank furrows (Figure 8b), which were observed on the flanks of the channel near the mouth, and are oriented parallel to the channel where the riverbank is sandy. In addition, channel oblique ripples (Figure 8c) were observed in the middle of the channel. The middle reach, which spans from the ICWW intersection (River km 2) to

approximately River km 7 (just down stream of the SH36 bridge), is dominated by low backscatter and an absence of bedforms (Figure 8d). The upper reach, above River km 7, is also dominated by high backscatter and relatively large bedforms including channel normal ripples (Figure 8e), located near River km 8.5, and large-scale scour pool bedforms (Figure 8f) near River km 10. Grain size analysis from surface sediment grab samples shows a similar tripartite distribution (Figure 9), where the riverbed of the upper and lower reaches are sand dominated and the middle reach is mud dominated. Consequently, the variations in backscatter are primarily a function of surface sediment textures.

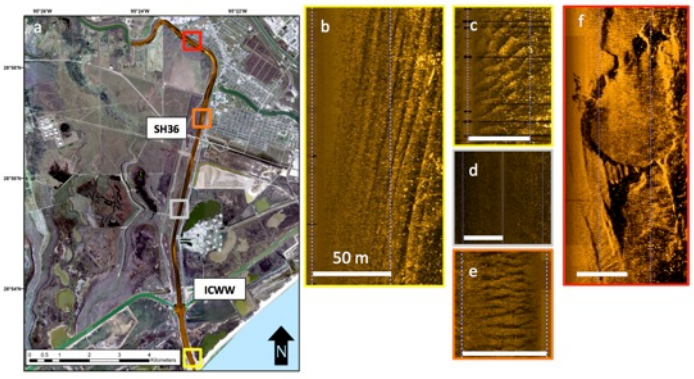

Figure 8: Side scan sonar (SSS) mosaic, lighter colors correspond to high backscatter. (a) Mosaic for the whole river, b-f are zoomed images of bedforms from different areas of the river. (b) Along-channel furrows from near the mouth, approximate location shown with yellow box in (a). (c) Mid-channel sand ripples from near mouth, location shown in (a) with yellow box. (d) Mid-river muddy area, location shown in (a) with grey box. (e) Up river mid-channel sand ripples, approximate location shown with orange box in (a). (f) Up river, large-scale bedforms, location shown in (a) with red box. Scale bars in b-f are equal to 50 m.

2.4.3 CHIRP Subbottom Data

The distribution of characteristics within the CHIRP data (Figure 10) follow the same tripartite distribution found within the SSS data. For majority of the survey, subbottom

penetration was poor, however some shallow subsurface features could be delineated. Within the upper reach of the study area, the CHIRP data (Figure 10b) show the riverbed to be dominated by large-scale bedforms, the high sand content created a hard surface reflector that inhibited deeper acoustic penetration. The mud dominated middle reach (Figure 10c) was devoid of bedforms, but demonstrated that the mud formed an acoustically transparent surface layer (10s cm thick) over a hard subsurface reflector. In the lower reach, near the mouth (Figure 10d), surface ripples were found overlying parallel, shallow subsurface reflectors.

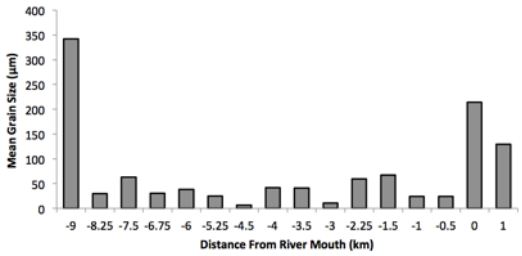

Figure 9: Mean grain size (µm) for surface sediment grab samples from May 2010 cruise. Negative values on x-axis correspond to distance up-river from mouth.

2.4.4 Bathymetry

Bathymetric data for the river were collected on May 17th and June 28th of 2010. Changes in bathymetry between these two surveys were calculated to quantify changes in bed elevation over time (Figure 11). Between these two surveys the change in bathymetry showed net deposition. The most significant area of deposition occurred between the ICWW (River km 2) and the SH36 Bridge (River km 6).

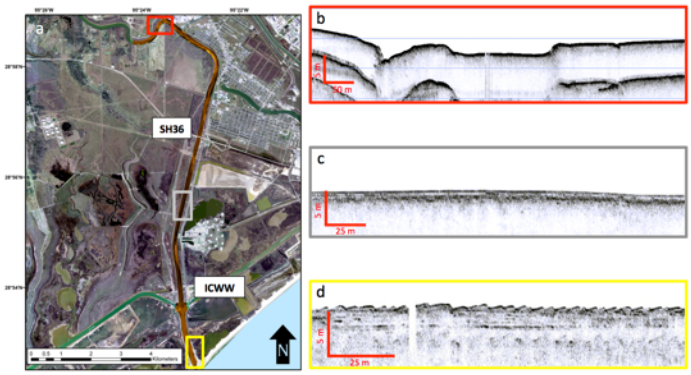

Figure 10: CHIRP subbottom profiles from August 2011. (b) Up river large-scale bedforms, location shown in (a) with red box. (c) Mid-river mud area, location shown in (a) with grey box. (d) sand ripples from area near river mouth, location shown with yellow box in (a). Vertical distances calculated assuming a speed of sound of 1500 m/s.

2.5 Discussion

The three distinct sedimentary zones observed within the lower Brazos River; sandy sediment, and bedforms observed near the river mouth and in the up river portion of the study area separated by a mud-dominated area that lacked bedforms, approximates a typical estuarine sedimentary zonation (Dalrymple et al., 1992). Therefore, the study area in the lower river defines the estuarine zone of the river, which also corresponded to the area where a salt wedge intrusion was observed in the river.

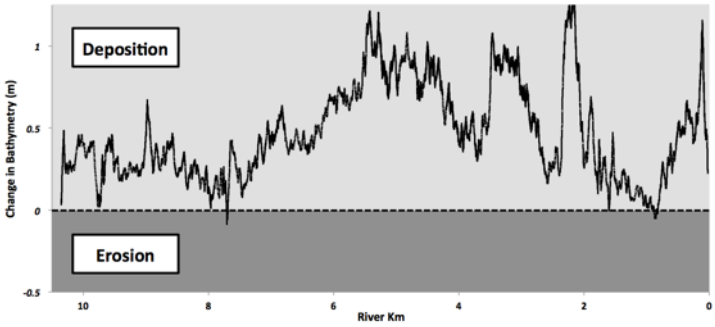

Figure 11: Change in bathymetry between May and June 2010 cruises. Data were constrained to the thalweg of the channel, positive values correspond to deposition, and negative values correspond to erosion.

For the Mississippi River, which the salt wedge intrusion has been previously studied, in part due to the weak tides, the limit of the intrusion is controlled primarily by the discharge of the river (Galler and Allison, 2008; Soileau et al., 1989; Wright, 1971). At the mouth of the Brazos River, the tidal range is similar, and the observations from this study also suggest the extent of the salt wedge intrusion to be a function of fluvial discharge, where at lower discharge the salt water extends further up river >14 km compared to 6 km for an average discharge, and no observed intrusion for elevated discharge. It should be noted that most of the sampling occurred during the ebb tide, the ebbing current would add to the river flow (Geyer et al., 2004), therefore the observed intrusion length likely represents the minimum landward extent. The one exception, October 2007, occurred during the slack waters of the low tide. Although the limit of the salt wedge intrusion likely varies over the tidal cycle, this is beyond the scope of this study, and from these observations we can conclude that for the Brazos River, discharge is the primary control on the salt wedge intrusion.

With the salt wedge present in the river, estuarine controls on the suspended sediment load occur, trapping sediment within the estuarine zone of the river. The trapping of the sediment was most notably observed in May 2010 (Figure 5a) with increased SSC confined to the freshwater portion of the river above the salt wedge, and no observed buoyant plume exiting the river mouth. Where the salt wedge was observed corresponded to the muddy middle reach observed in both the SSS and CHIRP data. These results suggest the trapping of suspended sediment creates the mud layer observed in the middle reach of the study area. The thickness and extent of the layer, as determined from the CHIRP data (Figure 12), spans from above River km 1, to upstream of the SH36 bridge, just past River km 8, with an average thickness of approximately 0.3 m. Galler and Allison (2008) observed a similar feature in the Mississippi River and concluded that this ephemeral mud layer was formed when fluvial suspended sediment flocculated, and rapidly settled after interacting with the salt wedge. The similarity between the observations on the Mississippi and Brazos Rivers suggest a similar mechanism, namely enhanced settling due to flocculation as the sediment interacts with the salt water in the lower river. This can explain the observation during the May 2010 sampling that showed a 2 – 3 fold decreases in SSC between the fresh water and underlying saltwater, suggesting that as the sediment interacted with the saltwater, flocculation occurred, and it rapidly settled thereby lowering the observed concentrations.

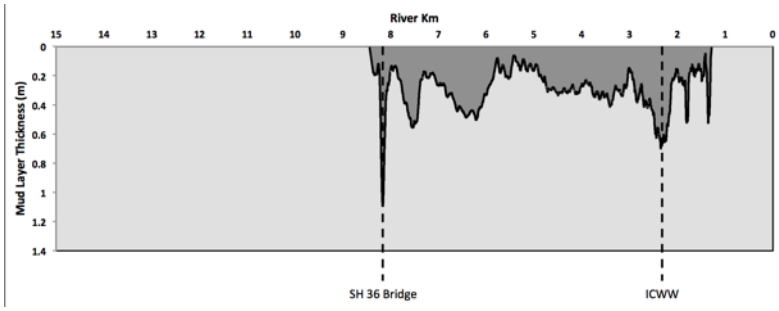

Figure 12: Thickness of the transparent mud layer from CHIRP data (example shown in Figure 10c)

Deposition was also observed as the change in bathymetry between May and June 2010, a time when the salt wedge was present in during both surveys, and a noticeable decrease in SSC was observed (Figure 5). This suggests that the salt wedge trapped sediment, reducing the SSC of the river by depositing the sediment in the muddy middle reach. The average change in bathymetry was approximately +0.4 m, and from this an average accumulation rate was estimated to be approximately 8 mm/day, calculated by dividing the average change in bathymetry by the time elapsed between measurements. Although this rate assumes constant deposition throughout the elapsed time period, it is comparable to the 2-9 mm/day Galler and Allison (2008) observed for the Mississippi River by short-lived radionuclides.

The mud layer in the Mississippi River was observed to be an ephemeral feature that was completely remobilized during the spring freshet (Galler and Allison, 2008). Evidence for remobilization of the mud layer in the Brazos River was also observed during this study. The OBS saturation layer that was observed during the increased discharge event on January 31, 2012 (Figure 6a) corresponded to the location of the mud layer. This

suggests that remobilization of sediment in the mud layer as river discharge increased contributed to extremely high SSC observed within the OBS saturation layer. This remobilization increased SSC beyond the source conditions of the river similar to what was observed on the Amazon River with extremely high near bottom SSC described as fluid muds (Kineke et al., 1996).

During increased discharge, observations showed the salt wedge to be pushed seaward of the river mouth, establishing the estuarine zone on the shelf proximal to the mouth. It is during this time that sediment can be exported from the river to the Gulf of Mexico. Therefore, a threshold can be estimated between sediment storage when the salt wedge is present in the river, and export to the Gulf of Mexico when the salt wedge is absent. Based on the observations in this study the highest discharge where a salt wedge was present, limiting export of sediment was approximately 260 m^3/s observed on October 13th, 2007. The lowest discharge where the salt wedge was absent from the river was observed on January 31st, 2012 at a rate of approximately 330 m^3/s. These observations suggest that at some discharge between 260 m^3/s and 330 m^3/s the salt wedge pushes out from the lower river, initiating export of sediment to the Gulf of Mexico.

Sediment export to the Gulf of Mexico was observed during the July 12th, 2007 and January 31st, 2012 cruises (Figures 4a and 6a) in the form of a buoyant plume. In addition to the buoyant plume observed during these export events, elevated SSC were also observed near the bottom below the buoyant plume. This may result as the

sediment settles toward bottom, it remains in suspension due to wave boundary layer processes (Grant and Madsen, 1986). The sharp reduction in SSC in the buoyant plume with increased distance from the river mouth as shown in Figure 7 while the buoyant plume extends for kilometers away from the mouth, provides evidence for rapid settling of sediment out of the buoyant plume. However, transport within a wave boundary layer suggests that sediment may be transported increased distances than would be dictated by settling alone.

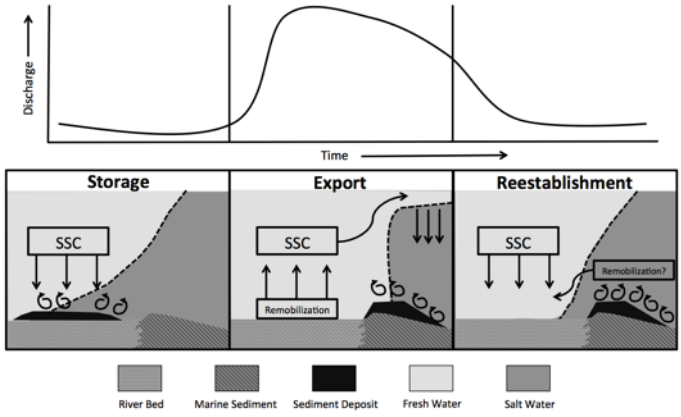

Figure 13: Conceptual model of observations made during this study. Top panel shows an idealized hydrograph of the river. Bottom panels show the the three lower river modes observed in the study, dotted black lines delineate the 10 PSU isohaline.

2.5.1 Sedimentation Model

Based on the observations of this study a conceptual model of sedimentation can be developed to describe fluvial sedimentation for the Brazos River as it relates to a salt wedge intrusion, specifically when sediment is trapped and stored in the lower river, and when it is exported to the Gulf of Mexico. As the results of this study suggest, the salt

wedge intrusion is primarily a function of river discharge, thus the model can be constrained by an idealized hydrograph. Therefore river flow conditions which include the rising and falling limbs have been divided into three modes: 1) lower river sediment storage, 2) lower river sediment export, and 3) salt wedge re-establishment (Figure 13).

Lower River Sediment Storage

This mode occurs during the rising limb of the river's hydrograph, or when estuarine conditions are present in the lower river. The salt wedge is present, and suspended sediment is trapped by the salt wedge, and subsequently stored within an ephemeral mud layer. During this time, the export of sediment to the Gulf of Mexico is negligible. However, the relative quantity of sediment trapped and stored during this time will be variable given the fluvial conditions.

The rating curve (Figure 2) shows a strong positive correlation between discharge and SSC suggesting that more sediment will be transported to the estuarine zone as the discharge approaches the export threshold. However, there is also a pronounced variability within the data observed in the rating curve. SSC for a discharge of 200 ± 5 m^3/s ranged from 98 mg/l to 1650 mg/l. This variability in SSC with similar discharge was also observed in this study. In October 2007 (~260 m^3/s) SSC in the river was generally less than 50 mg/l, and in May of 2010 (~220 m^3/s) SSC were typically about 200 mg/l. This suggests variability in the upstream sediment source, independent of discharge. Therefore, while river discharge may determine whether the salt wedge is

present in the lower river, quantifying the amount of sediment trapped will depend on other factors.

Lower River Sediment Export

As river discharge increases to a threshold between 260 m^3/s and 330 m^3/s, the salt wedge is pushed seaward of the mouth-bar crest establishing the estuarine zone seaward of the river mouth. At this time the lower river transitions from storage to export as suspended sediment is exported to the Gulf of Mexico. Sediment is exported via a buoyant plume to the Gulf of Mexico. During the export mode, sediment in the ephemeral mud layer can be remobilized and exported as well. The amount of sediment exported under these conditions will be a function of sediment availability from both the upstream supply and the mud layer, and the duration in which the discharge remains above the export threshold.

Reestablishment

During the falling limb of the hydrograph, the lower river transitions to a reestablishment mode, where the salt wedge reestablishes in the lower river. This mode is the least understood given the data, but potentially creates a mechanism in which sediment may be advected into the river from offshore as the salt wedge intrudes back up into the lower reach of the river. Data from October 2007 (Figure 4b), which represents the falling limb of the summer 2007 flood, showed the highest SSC were found at the mouth, near the bed, ~100 mg/l, within the salt wedge. This elevated SSC suggests a

supply of relatively fine grained sediment that was remobilized as a result of either classic estuarine turbidity maximum processes (Postma, 1967), or increased bottom stresses corresponding to decreased water depths in this area. Although the precise mechanism for resuspension cannot be determined from the data, the implication is that a mud deposit was formed seaward of the mouth; likely the result from the preceding flood which relocated the estuarine zone out of the river, on the shelf, for a prolonged period of time. As the salt wedge becomes reestablished within the river during the falling limb of the hydrograph, remobilization of the shelf mud deposit, via wave and or tidal activity, may advect sediment from offshore back into the river. Therefore, as discharge falls, and the estuarine zone moves from offshore back into the river, if sediment is available, there is potential to transport sediment from the ocean into the river.

2.5.2 Implications for Export of Terrestrial Material to the Ocean

The results of this study have identified a discharge threshold for the Brazos River, some point between 260 m^3/s and 330 m^3/s, which defines when sediment is exported to the Gulf of Mexico. Based on discharge data from the Richmond Gage station, the lowermost gage with the longest consistent record, since 1960 the 260 m^3/s threshold was exceeded 24% of the time, while the 330 m^3/s threshold was exceeded 19% of the time. This suggests that sediment export from the river is an infrequent event, and that over 75% of the time estuarine conditions exist in the lower river where sediment is being stored in the river, as an ephemeral mud layer. Although similar estuarine controls

of fluvial suspended sediment have also been observed in the Mississippi River, where the Brazos River differs is in its lack of a seasonal flood wave. In the Mississippi River the ephemeral mud layer was completely remobilized and exported during the spring freshet (Galler and Allison, 2008). With the absence of an annual freshet to completely purge the stored sediment, the potential for sediment to be added to the mud layer over multiple years exists, suggesting a regional climatic control on export. Evidence for this regional climatic control on sediment export was discussed in previous research focusing on Brazos River mouth bar formation following flood events, which found that these bars formed not with every flood event, but rather those events that were preceded by prolonged drought (Fraticelli, 2006) suggesting that the amount of sediment exported will vary depending on climatic cycles. Therefore, when an event does occur that can completely remobilize the mud layer the total sediment load exported will also be a function of the time elapsed since the previous event.

On a global scale these result highlight the importance of understanding the processes at river mouth to accurately predict terrestrial fluxes to the coastal ocean. Specifically these results show that for these types of rivers, where sediment export is modulated regional climatic cycles, the sediment load of the river may not be completely transferred to the ocean on an annual basis. Therefore the Brazos River may offer a credible model for other small to moderate sized rivers that do not have an annual freshet, to show the variability in sediment export that may allow for better estimates of the annual flux terrestrial material to the global ocean.

2.6 Conclusion

This study observed that suspended sediment in the lower Brazos River is modulated by the presence or absence of a salt wedge intrusion. During much of the time a salt wedge is present in the river, creating an estuarine zone in the lower river. Under these conditions, the salt wedge traps and stores suspended in an ephemeral mud layer in the middle reaches of estuarine zone. As discharge is elevated the salt wedge is pushed out of the river allowing sediment to be exported to the Gulf of Mexico. Based on the observations from this study the discharge threshold where a salt wedge is no longer present in the lower river occurred between 260 m^3/s and 330 m^3/s, which has occurred only 20 – 25 % of the time. When the threshold is exceeded sediment is exported to the Gulf of Mexico as a sediment plume. Because the Brazos River does not exhibit an annual freshet, regional climate variability will greatly influence the annual sediment flux to the coastal ocean, and it may serve as a model for similar rivers, which may affect global terrestrial sediment flux budgets.

3 EVENT DRIVEN DELTAIC SEDIMENTATION ON A LOW GRADIENT, LOW ENERGY SHELF: AN INVESTIGATION OF SEDIMENT ACCUMULATION ON THE BRAZOS RIVER SUBAQUEOUS DELTA

3.1 Introduction

Rivers serve as the predominant conduit to transport terrestrial material, both particulate and dissolved, to the global oceans (Milliman and Meade, 1983). Upon entering the ocean, marine processes can subject riverine sediment to alteration via periods of deposition, resuspension, and secondary transport prior to preservation in the stratigraphic record (Wright and Nittrouer, 1995). This establishes a distinction between sediment deposition, a relatively short-term process, and longer-term sediment accumulation. With an estimated annual flux of 20 billion tons of fluvial sediment reaching the worlds oceans (Milliman and Syvitski, 1992), understanding the fate of fluvial sediment in the marine environment, both in terms of deposition and accumulation, is important for a variety of processes that link terrestrial and oceanic systems, including organic carbon cycling (Bianchi and Allison, 2009) and the creation of the geologic record (Nittrouer et al., 1996).

The previous studies that have focused on the dispersal to, and subsequent accumulation of fluvial sediments in the marine environment include a variety of river systems, oceanographic settings, and geologic controls. These studies have included high sediment yield rivers, including the Amazon (Dukat and Kuehl, 1995; Kuehl et al., 1986; Nittrouer et al., 1996), Ganges-Brahmaputra (Goodbred et al., 2003; Kuehl et al., 1997),

and the Changjiang-Huanghe (DeMaster et al., 1985; McKee et al., 1983; Nittrouer et al., 1984a), which the combination of high sediment loads and relatively energetic oceanic conditions form subaqueous delta clinoforms on the mid shelf, removed from the river mouth. The Mississippi-Atchafalaya River system (Adams et al., 1987; Allison et al., 2000; Corbett et al., 2006) similarly has a high sediment load, but sediment accumulates adjacent to the river mouth due to the relatively quiescent oceanographic conditions of the Gulf of Mexico at the mouth. Small high-mountainous rivers located along active margins have recently drawn increased focus due to the disproportionately large sediment fluxes to the global ocean compared to their size (Crockett and Nittrouer, 2004; Farnsworth and Milliman, 2003; Kuehl et al., 2004). Additionally, a number of studies have also focused on the rivers draining into the Mediterranean Sea (Cattaneo et al., 2007; Frignani et al., 2005; Palinkas and Nittrouer, 2007) in which the sediment from multiple rivers can coalesce into a muddy shelf clinoform.

These previous studies on river systems throughout the world have contributed to a wealth of information on terrestrial sediment accumulation in the oceans. Compilation of this global data showed trends in how and where sediment accumulates, which allow for prediction about the fate of fluvial sediments from unstudied or understudied rivers based on the characteristics of their regional setting (Walsh and Nittrouer, 2009). One such understudied river is the Brazos River, located in the relatively quiescent oceanographic setting of the northwestern Gulf of Mexico. The Gulf of Mexico is where the greatest amount of sediment is discharged from the conterminous United States, and

the Brazos ranks second only to the Mississippi River in terms of sediment discharge to the Gulf of Mexico (Milliman and Meade, 1983). At the coast the Brazos River forms a relatively small delta that has been described as an asymmetrical wave-influenced delta (Bhattacharya and Giosan, 2003), punctuated by flood events (Rodriguez et al., 2000) , and regional climatic cycles (Fraticelli, 2006). These previous studies have primarily focused on morphological attributes of the subaerial delta. Bhattacharya and Giosan (2003) used the observed differences in beach ridges on either side of the subaerial delta to describe asymmetric wave-influenced deltas. Rodriguez et al. (2000) and Fraticelli (2006) both investigated the formation of mouth bars seaward of the river mouth following flood events, however to date not study has focused on sediment accumulation on the subaqueous delta.

Walsh and Nittrouer (2009) classified the Brazos River as a proximal-accumulation-dominated system, where the majority of the sediment should accumulate within a few kilometers of the coastline, proximal to the discharge location. One of the components that was unknown for the Walsh and Nittrouer (2009) analysis from the Brazos River was the distance to the nearest maximum shelf sediment depocenter. The purpose of this study is to better understand sediment accumulation on the Brazos River subaqueous delta in an effort to determine the nearest maximum shelf depocenter, which given the classification of this system by Walsh and Nittrouer (2009) should be located within a few kilometers of the mouth. The goals of this study therefore, are to describe and quantify sediment deposition and accumulation on the subaqueous portion of the Brazos

delta, proximal to the river mouth, and investigate changes in accumulation over the recent history of the subaqueous delta. This will be accomplished by analyzing data from sediment cores collected throughout an approximately 150-km^2 study area, centered at the mouth encompassing water depths from ~3 m to 15 m (Figure 14), and supplemented with high-resolution side scan sonar and swath bathymetry data. Ultimately, the sediment accumulation on the subaqueous delta will be compared to the sediment load of the river to better understand the fate of terrestrial material from the Brazos River.

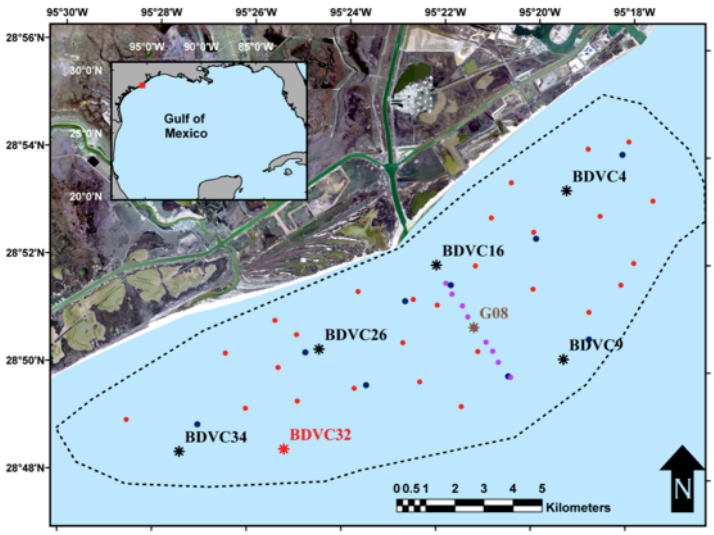

Figure 14: Base map showing study area outlined in black dashed line. Core locations over time are shown, gravity cores from 2007 (purple dots) some sites were reoccupied over time using gravity cores and box cores, 2011 box cores blue dots), and 2011 vibra-cores (red dots). Labeled cores marked by asterisks are specifically discussed herein, 2011 vibra-cores that were analyzed for geochronology (black asterisks), 2011 vibra-core analyzed for bulk density using the multi-sensor core logger (red asterisk), and brown asterisk denotes location of time series cores discussed.

3.2 Background

The Brazos River is the 11th longest river in the United States with an 118,000 km^2 watershed encompassing areas in northeastern New Mexico and large portions of Texas. It has the highest rate of flow and sediment yield of all Texas rivers (Rodriguez et al., 2000). Estimates of the sediment load for the river range from ~ 10 - 16 Mt/yr (Milliman and Syvitski, 1992; Syvitski and Saito, 2007), where the sediments are characterized by their distinctive red color derived from Triassic red beds (Rodriguez et al., 2000).

Annual rainfall in the watershed averages ~ 100 – 125 cm, although large deviations can occur during floods and tropical-storm induced precipitation events (Byrne, 1975). This is the only river on the Texas coast that consistently drains into the Gulf of Mexico where it forms a 35 km^2 delta of which approximately 70% is subaqueous (Rodriguez et al., 2000). The delta is located on a 130 km wide shelf with a 0.5 m tidal range and 1.1 m mean wave height (McGowen et al., 1977). Wave base for this part of the Texas coast is between 8 – 10 m (Siringan and Anderson, 1993). Net longshore drift is from the east to the west (Seelig and Sorensen, 1973). However, the direction of the longshore drift can fluctuate throughout the year as a function of wave direction, where waves from the southeast and from the south create a westward and eastward flowing longshore drift, respectively (Seelig and Sorensen, 1973). Most of the year the coastal current in this part of the Gulf of Mexico flows counterclockwise (east to west) from the Mississippi

River to the southern Texas coast primarily forced by wind stress (Curray, 1960; Nowlin Jr et al., 2005).

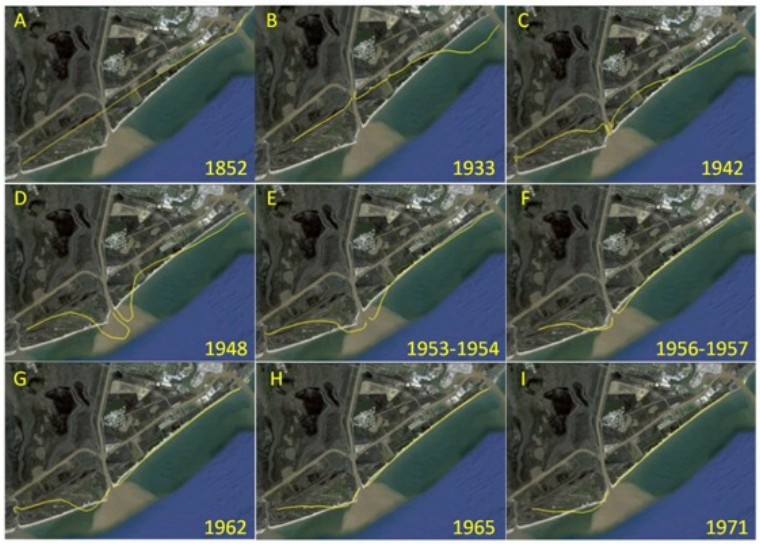

Figure 15: Historic shoreline position compared to 2009 satellite image. Modified from Seelig and Sorenson, 1973 and Google Earth. The 1852 shoreline (A) was prior to construction of the jetties at the old mouth.

The subaerial morphology of the delta is dynamic, and well documented. Arguably the most dynamic change occurred in 1929 when the US Army Corps of Engineers diverted the river mouth approximately 10 km to the southwest. Prior to the diversion of the river mouth, the river entered the Gulf of Mexico through what today is the Freeport Channel. The U.S. National Ocean Survey conducted a survey of the area in 1852 (Figure 15a). From this survey the Old Brazos Delta (OBD) largely resembled the present day configuration of Modern Brazos Delta (MBD), with an arcuate shape and a slight asymmetry favoring the down drift (western) lobe. Jetties were constructed starting in 1881 and completed in 1899, which caused the OBD to prograde approximately 1.6 km

seaward and develop a strong asymmetry to the west (Figure 15b). This asymmetrical deposition resulted from the jetties interrupting the longshore currents, allowing for river derived sediment to rapidly accumulate down drift of the jetties (Seelig and Sorensen, 1973).

In 1929 the river was rerouted to its present location, and the MBD began forming immediately. While the MBD was prograding seaward, the OBD was retreating landward at approximately the same rate (Figure 15c). By 1948 the subaerial MBD had grown almost 2.5 km in less than 2 years reaching its most seaward position, the subaerial delta exhibited a more cuspate shape, and at this time the river mouth was deflected approximately 45° eastward as shown in Figure 15d. After 1948, the MBD began to retreat landward, and by 1953 the OBD had returned to its approximate position in 1852 (Figure 15e and f). Hurricane Carla in 1961 made landfall approximately 100 km from the MBD as a category 4 hurricane, and the second most intense hurricane to make landfall on the Texas coast, ninth most on the mainland US as of 2006 (Blake et al., 2007). The storm reworked sediment at the MBD, skewed the shape of the delta to west (Figures 15g-i), and initiated a westward migration of the delta (Seelig and Sorensen, 1973). Only a slight asymmetry of the subaerial delta is evident today compared to past configurations in the 1940s and 1950s.

3.3 Methods

3.3.1 Geophysical Surveys

The surveys of the Brazos subaqueous delta, conducted in February and March of 2011, extended from near the Freeport Jetties in the east, to a few kilometers west of the mouth of the adjacent, and smaller San Bernard River. Side scan sonar and swath bathymetry data was collected concurrently using a 200 kHz Teledyne Benthos® C3D-LPM High-Resolution Side-Scan Sonar Bathymetric System. The survey area was constrained by the 3 and 10 m isobaths based on NOAA nautical charts; survey lines were spaced 100 m, and oriented parallel to the shore. The bathymetric data was corrected to mean low water (MLW) using NOAA tide station 8772447 located at the US Coast Guard station in Freeport, TX located approximately 10 km from the Brazos Delta study area.

3.3.2 Sediment Core Collection

Primary sampling occurred in September of 2011 where a total of 33 submersible vibra-cores, and 10 box cores were collected (Figure 14). The vibra-cores were 7.62 cm (3 in) in diameter, and on average recovered 1 m of sediment. These cores were collected using a pneumatic submersible vibra-core rig deployed off the stern of the vessel. Cores were stored upright and refrigerated until analyzed. Box cores were collected using GOMEX style box corer. Sediment splits were taken from the box corer using 15.24 cm (6 in) diameter PVC barrels, additional splits in plexiglass trays were taken for x-ray analysis.

Sediment cores had also been collected prior to the 2011 sampling cruise, starting in July of 2007 short (~ 30 cm length, 3.175 cm diameter) gravity cores were collected from stations located along a transect extending seaward from the river mouth during a flood event (Carlin et al., in review). Some of these sites were reoccupied overtime, October 2007, May 2008, July 2009, February and July 2010, during these times short gravity cores were collected with the exception of May 2008 when box cores were taken at the sampling sites.

3.3.3 Sediment Analysis

Vibra-cores were cut lengthwise, photographed, and visual descriptions of the sediment lithology were recorded. One-half of the core was archived for future reference and one-half processed for water content, grain size, and other analyses. Samples for water content analysis were sub-sampled in 1 cm thick sections for every centimeter in the upper 10 cm of the core, every other centimeter from 10 – 50 cm in the core, and every fifth centimeter below a depth of 50 cm. For grain-size analysis these cores were sub-sampled for every lithological unit as determined by visual analysis, sub-samples ranged from 1 – 5 cm thick depending on the unit. Both the box cores and the gravity cores were extruded, and sub-sampled at 1 cm thick intervals for the length of the core. The sub-samples were split for water content and grain-size analysis similar to the vibra-cores. All cores were x-rayed. The vibra-cores were x-rayed as half-rounds following being cut lengthwise and photographed, box cores were x-rayed using the split taken in

the plexiglass tray, and gravity cores were x-rayed in the barrels as full rounds prior to being extruded.

Water content analysis was preformed using wet samples of at least 10 g that were placed in pre-weighed aluminum dishes, weighed, and dried for at least 24 hours in an 80°C oven, and re-weighed after drying. Grain size analysis was performed with wet samples using a Malvern Mastersizer 2000® laser particle diffractometer. Sediment samples, ~3-5 g, were homogenized, combined with a dispersant, and sonicated to prevent and break-up flocs prior to analysis. In total the fraction of gravel (primarily small shells and shell fragments), sand, silt and clay were determined for each sample, as well as the mean grain size, further breakdowns in size distributions, and other statistical properties could be determined as needed.

3.3.4 Multi-sensor Core Logger/XRF Core Scanner

Additional analysis was performed on selected cores using a multi-sensor core logger to determine sediment bulk density, or an x-ray fluorescence (XRF) core scanner to measure relative elemental abundances down core. Seven vibra-cores were analyzed using the multi-sensor core logger at TDI-Brooks International Inc. in College Station, TX. Analysis was preformed on intact cores prior to the core being split. Measurements were made every centimeter for the entire length of the core. XRF analysis was preformed on two of the vibra-cores at the Integrated Ocean Drilling Program (IODP) core repository in College Station, TX using a third generation Avaa Tech XRF Core

Scanner. Measurements were made at energies of 10 kV and 30 kV, using a multichannel analyzer with a spectral resolution of 2048 channels at 20 eV/channel. Area under peaks in energy corresponding to specific elements was calculated to determine relative abundances. Archived sections of cores (split half rounds) were used for XRF analysis, with measurements being made every 0.5 cm down core for the length of the core.

3.3.5 Radionuclide Analysis

^{210}Pb activities were measured indirectly using the ^{210}Po method (Nittrouer et al., 1979; Santschi et al., 2001). Samples were wet sieved with a minimum amount of DI water through a 38-μm sieve, and the smaller fraction was used to minimize the influence of changes in available particle surface area on activity (Kuehl et al., 1986; Kuehl et al., 1989; Nittrouer et al., 1979). Aliquots (1g) of dried sample were spiked with a ^{209}Po tracer, which was added to the sample for yield determination, and were prepared by complete digestion with HCl, HNO_3 and HF. ^{210}Po and ^{209}Po were chemically separated and spontaneously deposited onto Ag planchetts (Santschi et al., 2001). Activity of the Po isotopes was determined by α-spectroscopy using a Canberra surface barrier detector. ^{210}Po is the granddaughter of ^{210}Pb and is assumed to be in secular equilibrium.

Sediment accumulation rates were determined by calculating a regression line using the equation:

$$A(z) = A(0)e^{(-\lambda z / S)}$$

where S = sediment accumulation rate, z = change in depth of the of the regression (cm), A_d = $^{210}Pb_{xs}$ activity at end of the regression (dpm g^{-1}), A_o = $^{210}Pb_{xs}$ activity at beginning of regression (dpm g^{-1}), and λ = radioisotope decay constant (^{210}Pb, 0.031 y^{-1}) (Bentley and Nittrouer, 1999; Nittrouer et al., 1984b).

^{137}Cs ($t_{1/2}$ = 30y; 662 keV peak) activity was determined using a low-background, high efficiency, high-purity Germanium (HPGe) planar γ-detector coupled to a multi channel analyzer. Samples were wet packed and counted for approximately 48 hours to determine the peak activity of ^{137}Cs in the core. ^{137}Cs was produced by bomb fallout as a result of atmospheric nuclear bomb testing in the 1950's and early 1960's, where peaks in activity correspond to peaks in atmospheric fallout in 1963-1964 (Krishnaswamy et al., 1971).

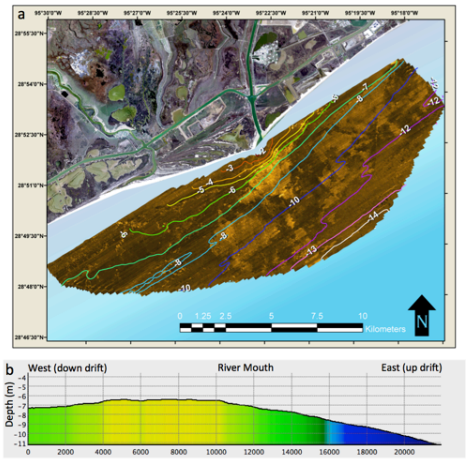

Figure 16: a) Side scan sonar mosaic with bathymetric contours in meters below mean low water. b) Bathymetric profile across the subaqueous delta from west to east showing the asymmetrical structure. Approximate location of the river mouth is labeled.

3.4 Results

3.4.1 Bathymetry

The bathymetry of the subaqueous delta (Figure 16) shows a distinct asymmetry up drift (east) and down drift (west) of the river mouth. On the up drift side, isobaths trend parallel to the shoreline and this area exhibits a relatively steep slope for the study site of ~1:625 or on average 0.09°. Down drift of the river mouth, water depths are shallower compared to the east, and only in depths less than 5 m do isobaths trend parallel to the shoreline. Measured water depths in this area of the subaqueous delta range from 2 m to 10 m below (MLW), with a slope of ~ 1:900 or on average ~0.07°. From Figure 16b, a bathymetric profile along the subaqueous delta clearly shows the asymmetry of the subaqueous delta. A diversion between the bathymetry data collected and the nautical chart used to plan the survey is evident as the survey area was constrained by the 10 m isobath according to the chart, but soundings in excess of 14 m were collected. This suggests that some areas have undergone erosion of upwards of 4 meters since the publishing of the nautical charts in 1938.

3.4.2 Side Scan Sonar

Results from the SSS showed a similar asymmetry as the bathymetry. The mosaic (Figure 17) shows three distinct areas with unique backscatter characteristics; the western area extends from the river mouth in a southwestwardly direction to encompass the majority of the western third of the survey area. This section is dominated by low

backscatter (darker colors) with small isolated areas of high backscatter (lighter colors). The central area encompasses the majority of the study area, extending eastward from the boundary of the western area across the other two-thirds of the study area, with a seaward boundary at approximately the 12 m isobath. Large, clearly defined high backscatter features dominate this area. The third area distinguished in the SSS mosaic is the southeastern area. Located to the southeast of the river mouth, this area is found seaward of the 12 m isobath, in the section of the study area where the deepest water depths were measured. The southeastern area exhibits higher backscatter than the western area, but lacks the clearly defined backscatter features of the central area.

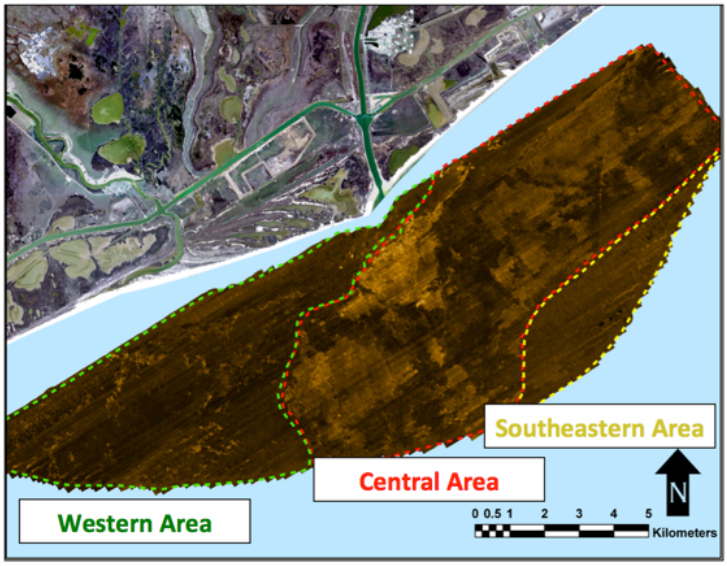

Figure 17: Subaqueous delta side scan sonar mosaic (lighter colors correspond to high backscatter). Three distinct areas based on backscatter characteristics are delineated by dashed lines; the western area (green), central area (red), southeastern area (yellow).

3.4.3 Sediment Core Data

Grain size analysis from the sediment cores showed that the sediment of the subaqueous delta is dominated by fine-grained sediments, primarily silts. Over 80% of all sediments analyzed were silt dominated with some clay (45% or less), and normally little sand (< 15%). Only in near-shore areas, landward of the 5 m isobath, did sandy sediments dominate the core. Where sandy sediment was present in cores, it was usually found as discrete layers on the order of a few centimeters thick. Increases in the number of these inter-bedded sand layers were primarily observed down drift of the river mouth within the western area (Figure 18).

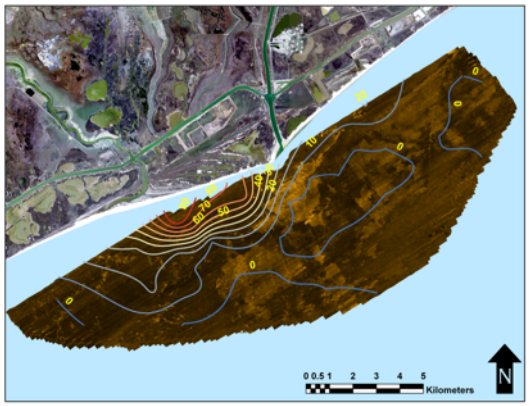

Figure 18: SSS mosaic with contours showing the percentage of sand dominated sediment with a core.

3.4.4 Sediment Color

Results from the vibra-cores, based on the visual descriptions, indicate that in addition to the grain-size of the sediments, the sediments also can be characterized by unique coloration. The colors observed range from grey to red, with variations in between

including brown, grey-brown, and red-brown (Figure 19). Variations in the color of sediment layers were previously observed by Rice (2009), where these five color classifications were established. The box cores and gravity cores were extruded, rather than split, so no visual descriptions were made, and thus no observations on the sediment color are available.

Figure 19: Range of colors observed within the sediment cores. Two end members were distinguished, grey and red, with variations due to mixing in between.

Figure 20a shows the percentage of the cores that were comprised of either grey or grey-brown sediment. The central area of the survey, as defined by the SSS, was relatively enriched in grey sediment, with a slight decrease in the far eastern section of the study area. However, the highest proportion of grey sediment was observed in the deep waters of the southeastern area. The proportion of grey sediment observed decreased both to the east, towards the Freeport channel and the OBD, and to the west in the western area. Grey sediment proportions are lowest proximal to the river mouth.

Brown sediment (Figure 20b) is relatively common throughout the study area, but dominate the nearshore areas both up drift and down drift of the river mouth. Although directly down drift of the river mouth values are relatively lower. In the central area the percentage of brown sediment in the cores generally decreases with increasing water

depth, with minimal brown sediment observed in the southeastern area. Most of the western area cores had over 40 % brown sediment.

The percentage of red sediment shown in Figure 20c consists of both red and red-brown sediment within the core. There are three distinct areas where red sediment dominates or comprise a significant portion of the sediment, one area in the far eastern edge of the study area proximal to the OBD, and two areas extending from the modern river mouth. The smaller of these two areas extends southeastward from the river mouth only a couple of kilometers, while the second extends southwestward, following the trend of the western area, approximately 5 km. Increases in red sediment in the east, proximal to the OBD, are likely relict sediment that was transported out of the old river mouth, as it now functions as a tidal inlet.

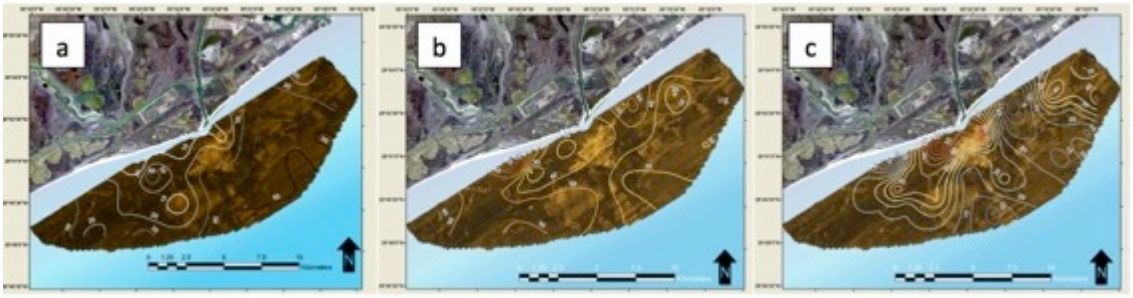

Figure 20: SSS mosaic with sediment color data. Percentage of sediment in the core that is classified as grey sediment which includes grey and grey-brown sediment (a), brown sediment (b), and red sediment including red and red-brown sediment (c).

3.4.5 Internal Sediment Fabric

In addition to layering distinguished by sediment color, layering was also observed within the core x-rays. X-radiographs reveal that all of the cores collected contained physical stratification. These stratified layers alternate between low x-ray intensity (dark), and high x-ray intensity (light) layers on a scale from mm to cm. Layers rarely exceed 10 cm in thickness.

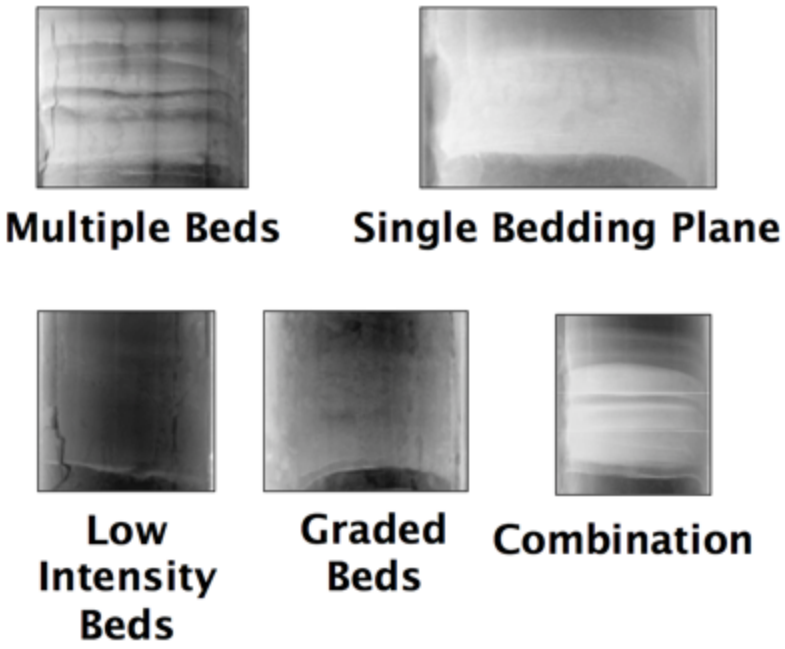

Figure 21: Various flood event bed types observed in the sediment core X-rays. The most common was the multiple beds type. Increased X-ray intensities correspond to increased sediment bulk densities.

Within the light layers, five distinct types were observed (Figure 21). A single bedding plane type consisted of a single light layer while the multiple beds type consisted of multiple light layers separated by sharp contacts. The low intensity bed type was brighter than the dark layers, exhibited sharp contacts at the top and base, but not as

bright as the single bedding plane or multiple beds types. A combination type consisted of a combination of a low intensity bed combined with a single bedding plane or multiple beds type. These four types all exhibited sharp contacts at both the top and the base of the layer, distinguishing it from dark layers above and below. The fifth type, the graded bed, had only one sharp contact at the base or top, and graded upwards or downwards respectively. However, this type was relatively rare.

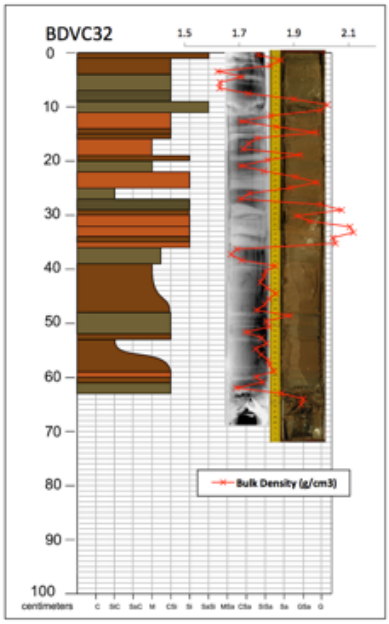

Figure 22: Example of core description, x-ray, core photo, and bulk density profile (g/cm^3) as determined from the multi-sensor core logger. In core description coloring refers to observed sediment color, width of layers correspond to grain size composition: C - clay, SiC – silty-clay, SaC – sandy-clay, M – mud (mixed silt and clay with little sand), CSi – clayey-silt, Si – silt, SaSi – sandy-silt, MSa – muddy-sand (mixed silt and clay with sand), CSa – clayey-sand, SiSa – silty-sand, Sa – sand, GSa – gravely-sand, G – gravel. Core location shown in Figure 14.

3.4.6 Sediment Bulk Density and Porosity

Data from the multi-sensor core logger, showed that sediment bulk densities measured ranged from ~1.4 to 2.2 g/cm^3. Relative increases in bulk density down core

corresponded to the light layers observed in the x-rays (Figure 22). The most significant changes in bulk density down core were the result of significant increases in the fraction of sand within a layer. No general trends of increasing bulk density with depth that might indicate relative changes in sediment compaction were observed, although it should be noted that the cores analyzed by the multi-sensor core logger were all less than 80 cm in length. Changes in sediment porosity down core, as determined through the water content analysis, also appeared to be controlled by changes in lithology, i.e. increases in sand correlates to decreases in porosity, rather than relative changes in sediment compaction from the top of the core to the base.

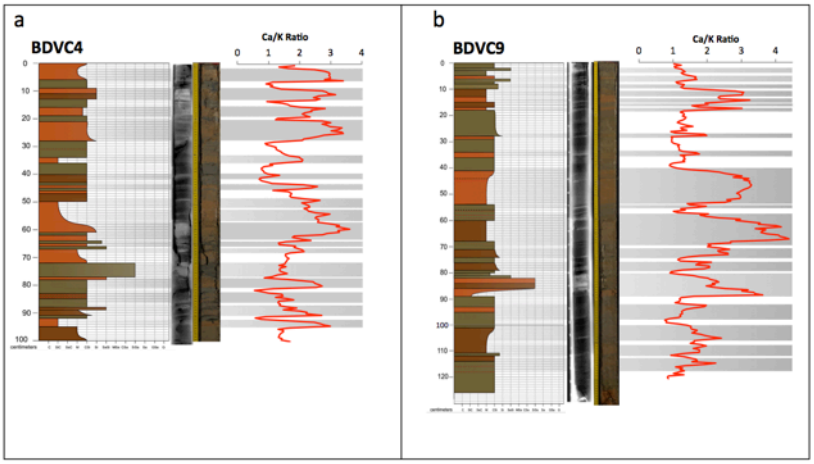

Figure 23: Core data from selected cores that include description, photograph, x-ray, radioisotope data and XRF data. Locations shown in Figure 21. Results include core description with layer color, and sediment size characteristics, core photos and x-rays. Horizontal bars indicate identified Brazos River layers. Graph shows Ca/K ratio (red line) from XRF analysis for cores a) BDVC4 and b) BDVC9.

3.4.7 XRF Data

Data from the XRF analysis is shown in Figure 23. Although a suite of relative elemental abundances were measured, Figure 23 shows the results of the ratio of calcium

to potassium down core. Individual profiles of elemental abundances reflect both changes in elemental composition as well as variations in sedimentary texture, core volume and artifacts. By using ratios of relative elemental abundances rather than the individual abundances, the systematic errors associated by variations in sedimentary fabric, core volume and artifacts are dramatically reduced (Rothwell and Rack, 2006). Changes in calcium abundances can show strong correlation with sedimentary units and are effective at indicating source material, for example biogenic carbonates (Croudace et al., 2006). This ratio was chosen to use calcium, normalized to potassium as a proxy for terrigenous clays in which potassium can serve as an interlayer cation, is widely available in soil clays (Simonsson et al., 2009), and the dominant source of terrigenous clay to the Gulf of Mexico is the Mississippi River (Balsam and Beeson, 2003; Sionneau et al., 2008). Therefore this ratio distinguishes the calcium-enriched Brazos River derived sediment, as the river drains the carbonate-rich areas of central Texas, from the calcium depleted, potassium enriched clay sediment derived from the Mississippi River. Rice (2009) showed through x-ray diffraction analysis that Brazos River derived sediment was relatively enriched in calcite, while non-Brazos, Gulf of Mexico sediment lacked calcite. For both cores measured, the profiles show pronounced peaks down core indicating layers relatively enriched in calcium. These layers vary in thickness from mm-scale to 10-20 cm. Some of the layers show a maximum at the base following an abrupt increase, and many exhibit multiple peaks within a layer of overall increased calcium.

3.4.8 Sedimentary Facies

From these results, sediment layers were distinguished as being derived from the Brazos River, or from the Gulf of Mexico (Figure 23). Primarily this distinction was made based on sediment color, internal sediment fabric, bulk density, and the Ca/K ratio. River derived sediments were generally toward the red end of the color spectrum (i.e. red or red-brown, but brown sediments could be included given the other parameters), exhibited high-intensity x-ray layers, relative increases in bulk density, and increases in the Ca/K ratio. Gulf of Mexico sediments therefore, were typically grey or grey-brown in color, lacked high-intensity x-ray layers, and did not show increases in bulk density or the Ca/K ratio. When including sediment texture results, three overall sediment facies were classified. Two are classified as being dominated by the Brazos River sediment, while the third consists of predominantly non-Brazos River, Gulf of Mexico sediment.

Proximal Brazos River Mouth Facies (PBRMF)

This facies consists of predominantly Brazos River derived sediment. As such the sediment has relative increased sand and coarse silt, is red, red-brown, or brown in color, has high x-ray intensity beds consisting of single bedding plane, multiple beds and combination bedding types, exhibit relative increases in bulk density, and is enriched in calcium. This facies is distinguished from the other river-derived facies because it consists of the relative increases in coarser-grained sediment (coarse silts and sand) that suggests it was deposited relatively close to the river mouth, near the source of the sediment.

Distal Brazos River Plume Facies (DBRPF)

The second of the river-derived facies consists of predominantly silt, relatively finer silt and increased clay content with low sand content, like the PBRMF it also exhibits red coloring, high x-ray intensity beds, although the beds in this facies are predominantly low intensity bed and graded bed types, increased bulk density, and increased Ca/K ratios. The primary distinction between this facies and the PBRMF is the relative increase in finer-grained sediment including fine silts and clays, with a relative depletion in sand. These observations indicate that this facies was deposited further away from the river mouth, potentially from sediment settling out of a buoyant plume, or winnowed sediment from deposits that were subsequently transported along or across the shelf.

Gulf of Mexico Innershelf Facies (GOMIF)

The third facies is interpreted to comprise the Inner Continental Shelf sediment of the Gulf of Mexico not derived from the Brazos River. This facies is composed primarily of silt, or a mixture of silt and clay and the beds associated with this facies are grey, or grey-brown in color, exhibit dark x-ray intensities that lack bedding, consist of low bulk density sediment, and low Ca/K ratios. This facies is interpreted to be shelf sediments transported to the study area by longshore currents from areas not impacted by Brazos River sediments.

3.4.9 Radioisotope Data

Five cores were analyzed for ^{210}Pb, and 4 cores were analyzed for ^{137}Cs (Figure 24). For ^{137}Cs three of the cores showed a peak in activity with depth in the core. In cores BDVC4 and BDVC9 the peaks were observed at a depth around 20 cm in the core, while BDVC26 the peak was observed at a depth around 75 cm. The fourth core analyzed, BDVC16, no ^{137}Cs peak was observed, rather only elevated levels near the surface were detected.

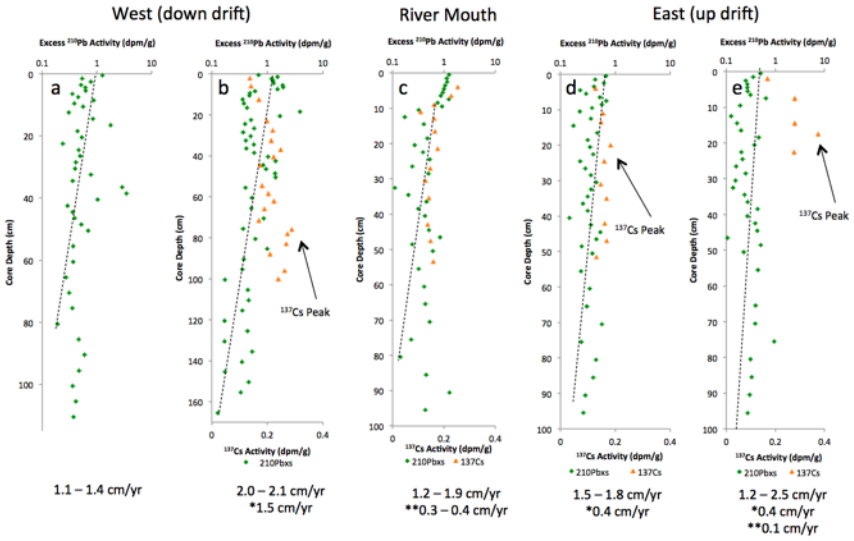

Figure 24: Down core profiles of ^{210}Pb and ^{137}Cs activities for a) BDVC34, b) BDVC26, c) BDVC16, d) BDVC9, e) BDVC4. Their relative location to the river is noted, and actual core locations shown in Figure 14. Text highlights estimated long term averaged accumulation rates as determined from ^{210}Pb activities, black dashed line indicates regression estimate, * represents accumulation rate since 1963 as determined by ^{137}Cs activities where available, ** represents accumulation rates in steady state surface layers from ^{210}Pb activities where available.

Measured ^{210}Pb activities for all of the cores do not appear to reach supported levels; this suggests that the sediment was deposited less than ~100 years ago. For analysis, a supported level of 0.85 dpm/g was assumed based on minimum activities detected.

Furthermore, for most of the cores logarithmic decay with depth indicative of steady-state accumulation was not observed. One exception was BDVC16, where the upper 10 cm exhibited steady-state accumulation. For the rest of this core, and throughout the other cores, activities were variable with depth, with peak activities often observed at depth below the surface. These results suggest non steady-state accumulation for much of the study area. Although non steady-state conditions were observed, general trends in decay with depth in the core were observed that suggest overall accumulation over time. Attempts to determine accumulation rates from regression lines were not successful as R-squared values were consistently below 0.25 for the vibra-cores.

3.5 Discussion

3.5.1 Event Sedimentation

The modern Brazos delta (MBD) formed in 1929 when the river mouth was diverted to its present location. Sub-bottom profile data from this area shows that there is a clearly defined deltaic clinoform that is between 1 and 5 meters in thickness (Carlin and Dellapenna, in review). The geochronology results from this study showed that none of the cores analyzed reached the background level of ^{210}Pb activities indicating that the sediments analyzed were deposited less than ~100 years ago. Furthermore, none of the cores analyzed, including those not analyzed for ^{210}Pb geochronology, exhibited a clear unconformity demarcating the boundary between the OBD and MBD strata This suggests the sediment recovered in the cores was deposited after the 1929 Brazos River diversion and only contain sediment from the MBD, yet without evidence for the

transition from the OBD to the MBD, it may be concluded that the entire MBD sequence is not represented in a single core.

The sediment data suggests that the subaqueous delta consists of alternating layers of Brazos River derived sediment and non-Brazos River, Gulf of Mexico sediment. Deposits from the river are on average approximately 3 – 4 cm thick, with the thickest observed being ~13 cm. The non-river derived layers were on average approximately 2 cm thick. The Brazos River deposits are hereby defined as fluvial-event layers, referring to a flood event within the river that transported fluvial sediment to the subaqueous delta. Non-fluvial layers therefore were deposited during times when fluvial sediment to the subaqueous delta was much lower, and background marine sedimentation dominated.

In addition, the subaqueous delta sediments also exhibits non steady-state accumulation (Figure 24), which demonstrates an absence of continual, i.e. seasonal or annual, accumulation over time suggesting temporal variation in the initial supply of ^{210}Pb activity to the area. This may result from variations in particle residence times in ^{210}Pb enriched waters, variations in particle surface area (a function of grain size), or changes in suspended sediment concentrations that would deplete dissolved ^{210}Pb for subsequent particles reaching the seabed (Kuehl et al., 1986). This has been observed in the sediments of other deltas including the Amazon (Dukat and Kuehl, 1995; Kuehl et al., 1986; Kuehl et al., 1995; Nittrouer et al., 1986b), the Ganges-Brahmaputra (Kuehl et al., 1997), on the shelf off the Eel River (Sommerfield and Nittrouer, 1999), in the Adriatic

Sea (Palinkas and Nittrouer, 2006, 2007), and in the Gulf of Papua (Palinkas et al., 2006). In these studies, areas that experienced non steady-state accumulation, also described as event sedimentation, occurred from unique conditions in the adjacent fluvial regime operating on seasonal or event time scales. These areas also exhibited physically stratified sediment layers within the x-rays with no evidence of bioturbation, similar to what is observed in this study. In addition, these areas were often located on the foreset regions of the deltas, or in other areas of relatively rapid accumulation.

Based on the observations of alternating fluvial event and non-fluvial layers in combination with the non-steady state accumulation observed in this study suggests that the Brazos River subaqueous delta is also dominated by event sedimentation. Sediment is supplied to the subaqueous delta during discrete events, with variable time in between events, but enough time to accumulate non-event layers. Recent work in the lower Brazos River suggests that potentially 75-80 % of the time a salt-water intrusion traps fluvial sediment in the lower river, preventing transport to the Gulf of Mexico that is controlled by regional climate variability (Carlin et al. in review). The pulsed nature of sediment export from the lower river offers a mechanism to explain an episodic supply of fluvial sediment to the subaqueous delta. Overall the fluvial-event layers represent 60 – 65 % of the sediment in the cores, suggesting that sedimentation is dominated by the fluvial event-scale sediment fluxes, which overtime have resulted in net sediment accumulation on the subaqueous delta.

3.5.2 Sediment Accumulation Rates

To determine sediment accumulation rates, given the non steady-state nature observed in the ^{210}Pb data, is difficult, but estimates can be made to offer a sense of relative rates to compare across different areas. Two different techniques were used to estimate accumulation rates from the ^{210}Pb data. These techniques provide overall average rates, which precludes small-scale changes in accumulation rates that may have occurred over time. First, because there was a general trend of net decay with depth in the core, accumulation rates were determined from changes in activity from the surface to the bottom, which has been shown to be effective in determining rough estimates of accumulation (Dukat and Kuehl, 1995). Secondly, accumulation rates were determined from the assumption that the length of the core had been deposited after 1929, as part of the MBD sequence. This is a conservative estimate, as the complete delta sequence was not captured within the core. Furthermore, on cores where ^{137}Cs activities show a peak in the subsurface of the core, accumulation rates were also estimated. These estimate the accumulation since 1963 (~past 50 years).

Overall net accumulation rate estimates are shown in Figure 24, ^{210}Pb-estimated rates for all five cores range from ~1.1 cm/yr to 2.5 cm/yr. These represent relatively rapid rates, which would be expected given the previous studies mentioned above that showed similar physical stratification observed in x-rays, and event-driven sedimentation. However, two of the cores, BDVC16 and BDVC4 did exhibit a zone of steady state decay at the surface, which rates calculated in these intervals yielded estimates of 0.3 –

0.4 cm/yr and 0.1 cm/yr respectively. Similar rates (0.1 – 0.2 cm/yr) were also observed in the upper sections box cores collected in 2008, a few kilometers seaward of the river mouth (Strauss et al., 2012), at stations reoccupied as part of this study.

Accumulation rates determined from peak ^{137}Cs activity were calculated for three cores (Figure 24). This yielded rates of ~1.5 cm/yr for BDVC26, and ~0.4 cm/yr for both BDVC9 and BDVC4. These accumulation rates suggest that for most of the deltaic record analyzed, sediment accumulated rapidly, however over the past couple of decades, ^{137}Cs results suggest that accumulation has slowed, slightly down drift of the river mouth, and dramatically up drift.

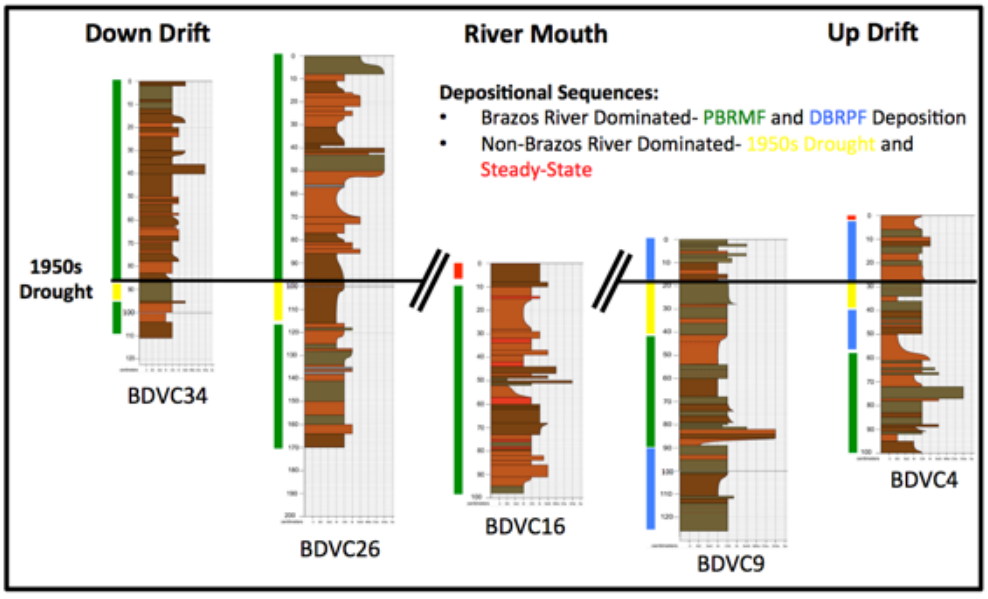

Figure 25: Cross-section with depositional sequences. Brazos River dominated sequences include PBRMF (green) and DBRPF (blues) deposition. Non-Brazos River dominated include the 1950s drought (yellow), and steady-state (red). The 1950s drought layer was not observed in core BDVC16.

3.5.3 Spatial and Temporal Trends in Accumulation

By analyzing the relative frequency and character of event layers within the cores, spatial and temporal trends in accumulation may be interpreted. In four of the cores, a period of decreased frequency of event layers was observed. This GOMIF-dominated depositional sequence was observed just below the ^{137}Cs peaks suggesting that these sediments were deposited prior to 1963. This sequence is believed to be the result of a period of prolonged drought that occurred throughout the Brazos River watershed for most of the 1950s. Similarly, a layer attributed to this climatic event has also been observed from benthic foraminifera data found in cores from the subaqueous delta (Strauss et al., 2012). Figure 25 correlates this sequence along the subaqueous delta, to compare relative rates of accumulation on both the up drift and down drift sides of the river mouth. One core, BDVC16, did not show evidence of this sequence, however a disconformity, at the base of the steady state layer (a depth of ~ 10 cm), suggests this sequence had been eroded. In addition Figure 25 shows the changes in observed Facies down core. The down drift cores (BDVC34 and BDVC26) are dominated by PBRMF deposition. At the river mouth (BDVC16), the sediment below the observed disconformity is also primarily PBRMF. Up drift, cores BDVC9 and BDVC 4, exhibit changes with DBRPF deposition above the 1950s sequence, and both PBRMF and DBRPF below.

This data show two distinct sediment accumulation phases of the MBD: before the drought when sediment accumulated rapidly throughout the entire delta, and after the

drought when sediment accumulation is predominately down drift of the river mouth. These phases are consistent with the subaerial changes to the delta over time (Figure 15), and as the PBRMF is distinguished by increased sand content, critical for delta progradation (Kim et al., 2009), this suggests that areas and periods of progradation correspond to PBRMF facies dominated sediment. At the river mouth, erosional evidence is present as seen in the disconformity in core BDVC16, and throughout the central and southeastern areas accumulation rates have slowed, approximating relative sea level rise for the region (Kolker et al., 2011). Accumulation rates approximating relative sea level rise suggest equilibrium between the sediment supply and sediment reworked by marine process, where accumulation occurs only due to the increase in accommodation space provided by the increase in relative sea level (Nittrouer et al., 1996). Relative dominance of marine processes reworking the sediment of the central and southeastern areas may explain the increases in grey and grey-brown sediments observed within these areas (Figure 21a). Figure 25 suggests that following the drought in the 1950s, marine processes may dominate over fluvial sediment supply, as accumulation of sediment has primarily been down drift of the river mouth. To this point, this second phase of accumulation on the subaqueous delta predominantly down drift of the river mouth following the drought is in agreement with ^{137}Cs sediment accumulation rates.

The event-driven sedimentation with a lack of bioturbation is typical of deltaic foresets, while deltaic topsets are typically accumulation limited beyond changes in

accommodation space (Walsh et al., 2004). This would suggest, that up drift of the river mouth, where event sedimentation has transitioned into accommodation space limited accumulation, represents a transition from foreset deposits to topset deposits that has occurred over the past 50 years. However, the dramatic changes in the shoreline position of MBD after formation (Figure 15) suggest that this area does not approximate a typical prograding delta clinoform transitioning from foreset to topset, but possibly abandonment of the clinoform. While the periods of shoreline progradation were likely coupled with the periods of rapid accumulation on the subaqueous delta and typical progradation of the delta clinoform, these periods of shoreline retreat likely correspond to the observed dramatic reduction in the accumulation rates, and potentially erosion or abandonment of the clinoform. The combination of changes in shoreline positions and accumulation rates, spatially and temporally suggest the primary depocenter has shifted over time. For example, prior to the drought in the 1950s the primary depocenter may have been located at the river mouth or even slightly up drift of the river mouth, evidence for which is observed in the southeastwardly trending red sediment depocenter seen in Figure 21c. After the drought, the data shows that the majority of the sediment is accumulating to the west of the river mouth suggesting an asymmetry in deposition. Furthermore, the asymmetric bathymetry of the subaqueous delta observed today (Figure 16b) also suggests preferential sediment accumulation down drift of the river mouth.

3.5.4 Preservation and Reworking of Fluvial-Event Layers

Evidence of asymmetric accumulation of sediment over the past 50 years on the subaqueous delta could result from unidirectional transport of fluvial derived sediments via longshore currents, or varying efficiency in the preservation of event layers across the delta. Although the dominant longshore current direction is to the west, the direction does switch throughout the year as a result of local wind directions (Curray, 1960; Nowlin Jr et al., 2005), thereby indicating bidirectional current flow over the course of the year.

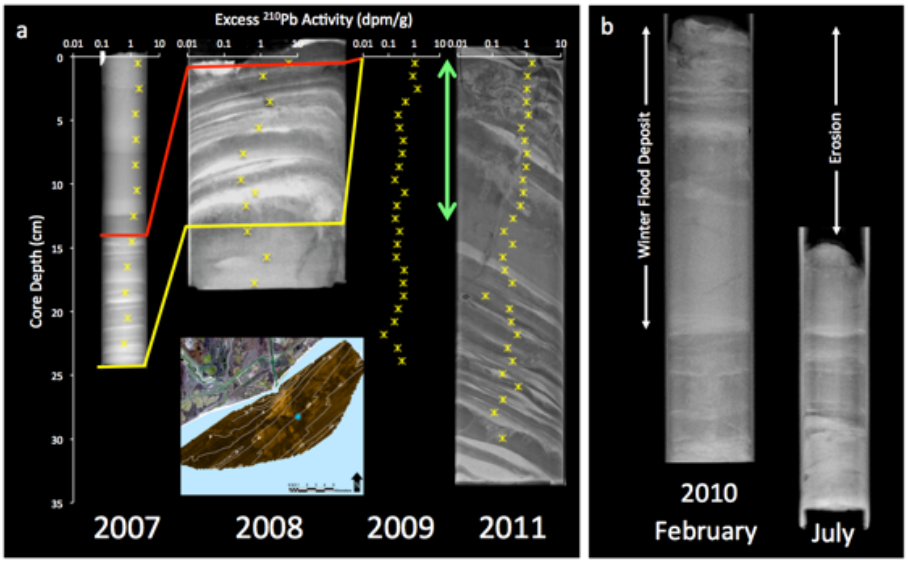

Figure 26: Time series data form 2007 to 2011. Location shown in inset. a) X-rays and Excess ^{210}Pb Activities (yellow), no x-ray for the 2009 core. Lines correlating layers, 2007 flood deposit in red, green arrow indicates bioturbation. Sloping strata in 2011 x-ray is an artifact of box coring, resulting from the box corer entering the seabed at an angle. b) X-rays from February and July of 2010 showing erosion of a winter flood deposit.

By reoccupying coring locations overtime, we were able to investigate the preservation of event layers in the stratigraphic record at a specific site on the delta. Figure 26 shows

data from a coring location approximately 4 kilometers from the river mouth starting after the 2007 flood, and subsequently reoccupied at least once a year through 2011. The 2007 flood deposit was approximately 15 cm thick and consisted of uniform ^{210}Pb activity and nearly uniform x-ray intensities. Similar characteristics in flood deposits have been observed for both the Eel (Sommerfield and Nittrouer, 1999; Wheatcroft et al., 2009) and Po river shelves (Palinkas and Nittrouer, 2007). The flood deposit contrasts with the underlying sediment, which exhibits the physical stratification similar to what was observed in the vibra-cores throughout the delta. In the May 2008 core, when the site was reoccupied there is no evidence of the 2007 flood deposit below the surface, suggesting almost complete remobilization of the flood deposit in less than one year. The core collected in July of 2009 followed the passage of Hurricane Ike in September of 2008, which made landfall approximately 60 km east of the study area. Although no x-ray was available for this core, correlation with ^{210}Pb activities show that an additional 13 cm of erosion occurred at the study site, potentially the result of the storm. When the site was reoccupied in September of 2011, correlation to past cores was difficult due to the presence of an approximately 10 cm surface mixed layer due to bioturbation. Evidence of bioturbation was also observed in some of the other cores collected in 2011, however this was the only time any such evidence had ever been observed while these stations had been reoccupied. In addition to annual changes, seasonal variability is shown in Figure 26b from cores taken in February and July 2010. Although no ^{210}Pb data are available for these cores, evidence from the x-rays show

partial erosion of sediment deposited during a February flooding event when the station was reoccupied in July of that year.

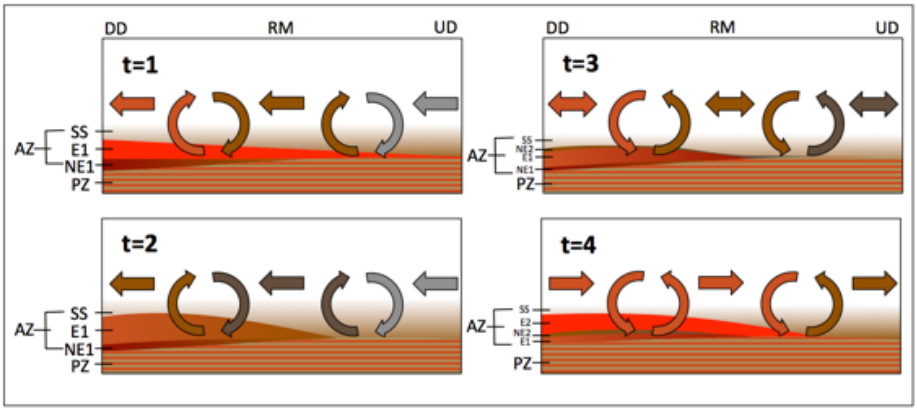

Figure 27: Conceptual model showing sediment mixing and sedimentation across the study area over four sequential time periods. Panels are a cross section across the subaqueous delta with the river mouth (RM) center and the Down drift (DD) left and Up drift (UP) to the right based on dominate longshore current direction. Sediment is divided into two zones, the active zone (AZ) where sediment is available for resuspension and remobilization, and the preservation zone (PZ) where sediments are no longer available for remobilization. The AZ is sub-divided into suspended sediment (SS), and event (E) and non-event (NE) layers. Straight arrows show current direction with sediment color. Circular arrows indicate sediment mixing with subsequent sediment coloring. Sediment is deposited throughout the delta, but preferentially accumulates down drift (modified from Rice, 2009).

These cores were collected from ~4 km directly seaward of the river mouth within the area of the subaqueous delta in which sediment accumulation scales with relative sea level rise. Overall the time series core data shows that, although this area is receiving fluvial sediment input during floods, and deposition of flood event layers, remobilization of the event layer is subsequently occurring. As a result, preservation of event layers in this area is low, which contributes to the low net accumulation that has been observed over the past ~50 years in this area. Furthermore the erosion observed potentially resulting from storm events may also describe the mechanisms responsible for clinoform

abandonment in this area. Observations following the impact of Hurricane Ike in 2009 suggest erosion during storm events is potentially greater than multiple years of sediment accumulation. The ~ 13 cm of erosion observed between 2008 and 2009 would require over 30 years of sedimentation to return to pre-storm conditions given the observed sedimentation rate of 0.4 cm/yr. However tropical storms affect the delta area on average once every two years (Byrne, 1975), making recovery in these areas following a storm from typical sedimentation difficult.

3.5.5 Conceptual Sedimentation Model

The preservation of event layers in the sediment record is a function of the time spent in in the active zone, where the sediment layers are subjected to mixing through physical and biological processes. Increased thicknesses and frequency of deposition of event layers "move" the event layer rapidly through the active zone, increasing preservation potential (Wheatcroft et al., 2009). Figure 27 uses a conceptual model to illustrate the nature of sedimentation of the Brazos subaqueous delta based on the results of this study. Modified from Rice (2009), the model shows that sedimentation is dominated by flood events. As the flood event deposits sediment throughout the subaqueous delta, its relative thickness along the subaqueous delta will reflect the direction of longshore drift at the time of the flood. Following initial deposition, sediment is remobilized, where the Brazos River derived red sediment is mixed with grey Gulf of Mexico and/or older sediment, diluting the red color. During prolonged periods between flood events shelf sediment is transported via marine processes from outside of the subaqueous delta,

creating non-Brazos River derived layers. For the portions of the delta up drift of the river mouth, marine processes completely remobilize event layers preventing preservation, and limiting accumulation. Repeated cycles of 1) fluvial-event deposition, 2) seabed remobilization, and 3) non-fluvial deposition create the physically stratified bedding observed. Down drift of the river mouth, increased accumulation "moves" the event layers out of the active zone to be preserved within the sedimentary record. The fundamental differences in this model compared to the one proposed by Rice (2009) is that accumulation is asymmetric across the delta, where accumulation is dominated down drift of the river mouth and limited up drift, and that mixing of sediment color occurs during remobilization and transport as opposed to deposition. This mixing regime is supported by the sharp contacts observed between layers in the x-rays, as opposed to more gradational contacts that would results from the mixing of newly deposited sediment with the underlying layer.

3.5.6 Sediment Budget

Sediment budgets for continental shelves proximal to river mouth incorporate numerous uncertainties and large errors, particularly for areas that exhibit non steady-state sediment accumulation (Kuehl et al., 1986), however they can be useful in understanding the fate of terrestrial material. The sediment budget calculated utilized the ^{137}Cs sedimentation rates therefore representing sediment accumulation over the past ~50 years (Figure 28). To determine the budget, sediment masses were calculated by multiplying the accumulation rates observed by the area, and an average dry bulk density

of 2.65 g/cm^3, then assuming an average porosity of 0.60, consistent with observations. The three areas delineated by the SSS, which had also exhibited unique sedimentation characteristics, defined aerial extents for the determination of the budgets. The annual sediment masses for each area calculated represented the sediment mass required to maintain the observed sedimentation rates. The sum these values were compared to reported estimates of the average annual sediment load of the river (Milliman and Syvitski, 1992) to determine the fraction retained within the study area.

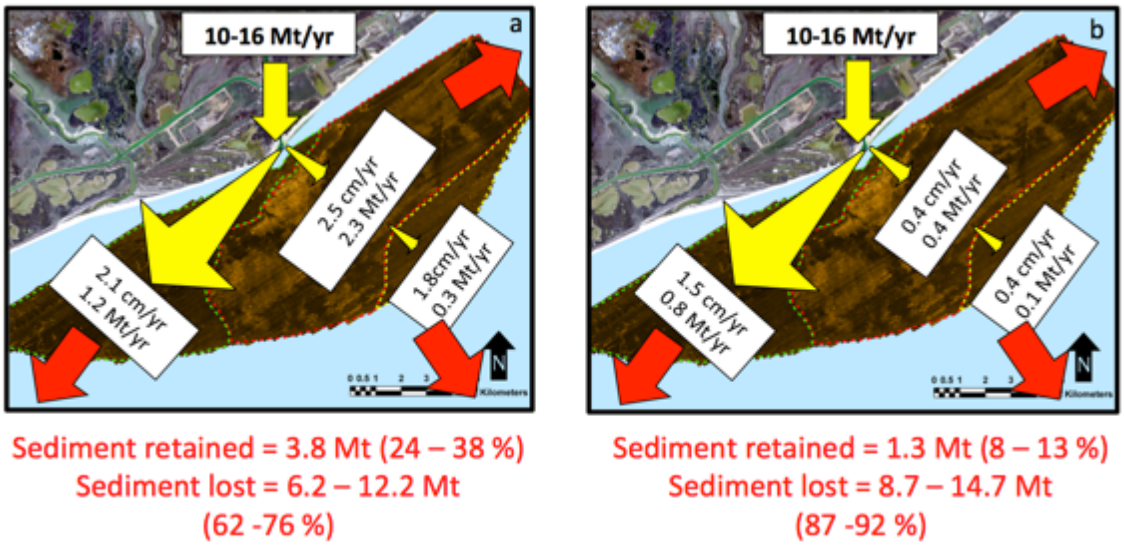

Figure 28: Sediment budget model showing annual sediment load partitioned into the 3 areas delineated by the SSS data and by deposition/accumulation characteristics. a) Budget based on long term averaged sediment accumulation rates. b) Budget based on accumulation rates over the past ~50 years. Red arrows indicate sediment loss from the study area.

Based on the accumulation rates over the past ~50 years the budget estimates only 8 – 13 % of the sediment load of the river is needed to maintain the accumulation rates measured. This sediment budget suggests that the majority of the sediment load of the

Brazos River (87 – 92 %) is bypassing the study area. It is important to note that this budget is based on a relatively small study area. However, Walsh and Nittrouer (2009) predicted that for the Brazos River, most of the sediment accumulation would be within a few kilometers of the river mouth, within the study area. Therefore only a small fraction of the sediment load is retained within the study area, and most of the sediment is bypassing the study area, and transported increased distances from the river mouth. If accurate, this would suggest the nearest maximum shelf depocenter may not be located with in the study area, and that the Brazos River does not fit into the proximal-accumulation-dominated model suggested for this river by Walsh and Nittrouer (2009). Recent work on the Atchafalaya River also diverges from the proximal-accumulation-dominated model suggested by Walsh and Nittrouer (2009) due to increased winter wave energy, which would approximate a subaqueous delta clinoform system (Kolker et al., in review). Similarly for the Brazos River, increased winter wave energy corresponds to times of relatively elevated river discharge (Figure 29). This may explain the deviation of the system from the Walsh and Nittrouer model, as flood events often correspond to times of increased wave activity, in which the system would approximate a subaqueous delta clinoform or marine dispersal system, where sediment deposits are removed from the river mouth. Recent studies have shown that an expansive mud blanket on the central Texas shelf has been forming over the late Holocene, which contains a large fraction of Brazos River derived sediments (Weight et al., 2011).

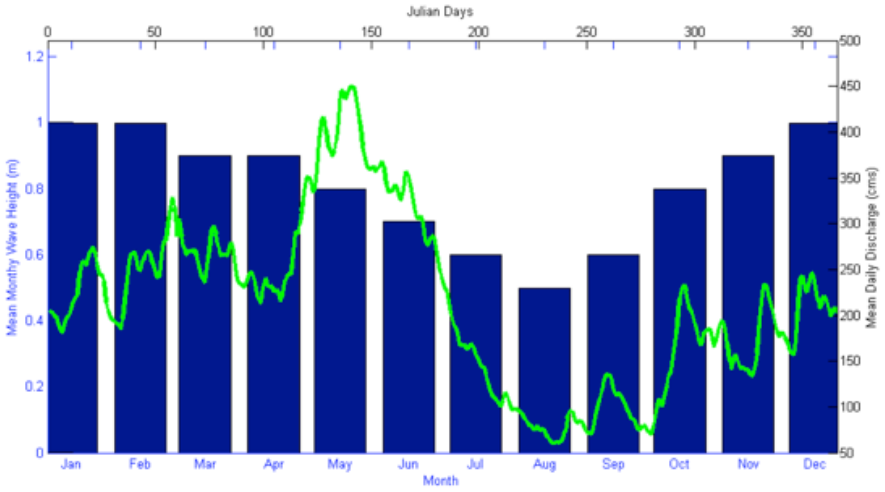

Figure 29: Graph of mean daily discharge of the river (m^3/s) over the coarse of the year (green line), and the mean monthly wave height in meters (blue bar) as measured from NOAA Buoy 42019 located approximately 60 NM from the study area. Discharge data courtesy of USGS Gage Station 08114000 at Richmond, TX.

3.6 Conclusion

Results from this study have shown that the subaqueous delta of the Brazos River proximal to the mouth is dominated by fluvial flood event sedimentation. Within the sediment record the fluvial event layers can be distinguished by sediment color, increased sediment bulk density, and mineralogy. Throughout the sediment cores, depositional sequences were classified as Brazos River and non-Brazos River dominated. The Brazos River dominated consisted of PBRMF and DBRPF deposition as distinguished by differences in relative sediment textures. Non-Brazos River dominated sequences (GOMIF) included a period of reduced frequency of fluvial-event layers, believed to be the result of a prolonged drought during the 1950s.

Although ^{210}Pb results yielded non steady-state accumulation characteristics, long term averaged accumulation rates were determined to be fairly rapid, between 1 – 2.5 cm/yr. These rates are consistent with the foresets of other subaqueous deltas or fluvial shelves, which exhibit similar event driven sedimentation. Over the past ~50 years, however, accumulation has largely been restricted to the areas down drift (west) of the river mouth, and much of the study area has been accumulating at rates comparable to relative sea level rise. Such a change traditionally would indicate a transition from foreset to topset deposition, however given the response of the shoreline at this same time, it may signal abandonment of that portion of the clinoform. Time series data shows a potential mechanism to describe abandonment where flood deposits in this area can be remobilized within a year, and net erosion can result from storm events. In addition, a sediment budget estimate concludes that the majority of the sediment load from the river is bypassing the study area. This suggests that the nearest maximum shelf depocenter for the Brazos River was not located within the study area. Therefore this system does not approximate a proximal-accumulation-dominated system that would be predicted given the oceanographic conditions, but rather may approximate a more oceanographic energetic system due to the timing of floods corresponding to times of increased wave activity.

4 EVOLUTION OF A MODERN DELTA: PROGRADATION/DEGRADATION, NATURAL/ANTHROPOGENIC ALTERATIONS AND CROSS-SHELF TRANSPORT ON THE BRAZOS RIVER DELTA, TX

4.1 Introduction

In 1929 the United States Army Corps of Engineers diverted the mouth of the Brazos River from its natural path. At the new river mouth, located approximately 10 km down the coast from its prior location, a new delta immediately began forming as sediment was dispersed into the Gulf of Mexico. This is not an isolated event as deltas throughout the world have increasing been impacted by human activity as a significant portion of the human population lives within deltaic coastlines (Syvitski, 2008). In addition to natural processes, the modern evolution of many fluvial-deltaic systems are now being shaped by anthropogenic forces including interventions to control the flow path of distributary channels, stabilization of banks, mitigation of the seasonal flood cycle, and crop irrigation practices (Syvitski and Saito, 2007). To date, human imprint on coastal environments has been under-appreciated (Syvitski and Kettner, 2011), and moving forward, understanding deltaic responses to both natural and anthropogenic forces will be critical not only to the environment, but to human populations.

At the interface between a river and the continental shelf fluvial sediments accumulate to form deltas. As a result the specific morphology of a delta is primarily influenced by such environmental conditions as river length, average maximum discharge, total

sediment load, suspended sediment concentration, accommodation space, tidal and wave energy (Syvitski and Saito, 2007). However, as waves are the primary mechanism in which deltaic sediments are reworked, the relative dominance of wave remobilization versus fluvial sediment supply will ultimately govern the geometry of a delta (Coleman, 1982). To this point, recent increased focus on fluvial dispersal systems has aided in the understanding that deltas are no longer confined to subaerial deposits, but also include the subaqueous deposits on the shelf that reflect the balance between sediment supply and the regional oceanographic conditions (Kuehl et al., 1997; Palinkas and Nittrouer, 2007; Walsh et al., 2004).

In addition to natural processes shaping delta morphology, human intervention has become an increasingly more important component. Human activities can alter sediment loads delivered to the delta, either by increasing the load, due to such interventions as changes land use, or reducing the number of distributary channels. Alternatively, sediment loads can also decrease due to interventions including surface water retention (damming), and diversion or removal for irrigation in arid regions (Milliman and Syvitski, 1992; Syvitski and Kettner, 2011). These activities occur throughout the fluvial-deltaic system. For example, the geomorphology of modern Po delta has been the result of human activities on the catchment, for instance deforestation, and to the delta, including levees, dikes and diversions (Correggiari et al., 2005; Trincardi, 2004). In the late 16th to early 17th centuries, Venetian technicians diverted the Po River to avoid sediments from closing the lagoon mouths in the Veneto region, but this diversion

cut off sediment supply to the "Renaissance delta" of the Po and initiated the formation of the "modern delta" (Simeoni and Corbau, 2009).

This study investigated the evolution of another "modern delta," the Brazos River delta. A "modern delta," as defined for this study, is one that has formed and evolved under the interplay between natural and anthropogenic forces. The Brazos River delta serves as an ideal study area to investigate the evolution of a modern delta, as the evolution of the "modern" subaerial delta is well documented. However little is known about the evolution of the subaqueous delta, primarily how it relates to the interplay between sediment supplied by the river, and the sediment reworked by marine processes. Through the use of high-resolution side scan sonar data, bathymetric data both historical and present, and shallow sub-bottom seismic data the morphology of the new subaqueous Brazos River delta was determined. The goal of this study is to combine these data with the history and evolution of the subaerial delta from historical photographs and imagery, to determine the modern deltaic response to natural and anthropogenic alterations to the system over time.

4.2 Background

The Brazos River is the 11th longest river in the United States with an 118,000 km^2 watershed encompassing areas in northeastern New Mexico and large portions of Texas. It has the highest rate of flow and sediment yield of all Texas rivers (Rodriguez et al., 2000). Sediment load estimates for the river range from ~ 10 - 16 Mt/yr, the second only

to the Mississippi River in terms of sediment delivered to the Gulf of Mexico (Milliman and Meade, 1983; Milliman and Syvitski, 1992).

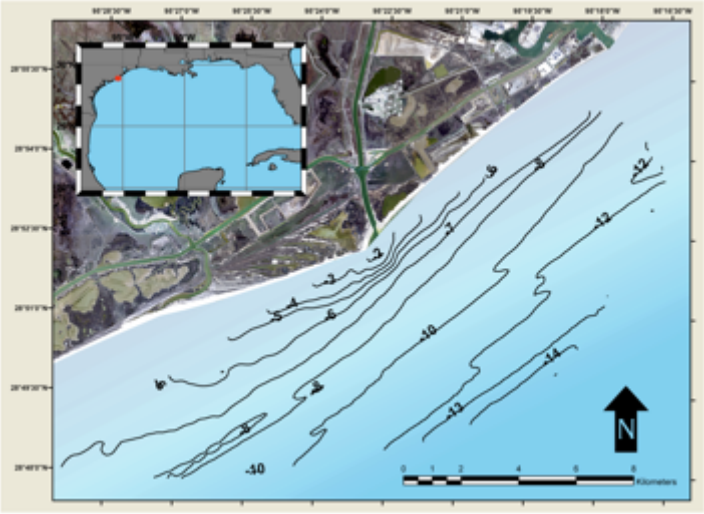

Figure 30: Study area with bathymetric data. Isobaths are in meters below mean low water.

Annual rainfall in the watershed averages ~ 100 – 125 cm, although large deviations can occur during floods and tropical-storm induced precipitation events which affect the delta area on average of once every two years (Byrne, 1975). This is the only river on the Texas coast that consistently drains into the Gulf of Mexico where it forms a 35 km^2 delta of which approximately 70% is subaqueous (Figure 30). The delta is located on a 130 km wide shelf with a 0.5 m tidal range and 1.1 m mean wave height (McGowen et al., 1977). Wave base for this part of the Texas coast is between 8 – 10 m (Siringan and Anderson, 1993). These waves generally trend northeast-southwest, approaching the shore in a northwest direction, resulting from predominately southeasterly winds (Rodriguez et al., 2000). As a result, net longshore drift is from the east to the west

(Seelig and Sorensen, 1973). Most of the year the coastal current in this part of the Gulf of Mexico flows counterclockwise (east to west) from the Mississippi River to the southern Texas coast. This nearshore current is primarily forced by wind stress. Beginning in May wind stress begins to change, causing the current to switch, flowing from South Texas towards the Mississippi River. This direction persists through the summer months, primarily July and August, and by September both the wind stress and currents have returned to a counterclockwise flow (Curray, 1960; Nowlin Jr et al., 2005).

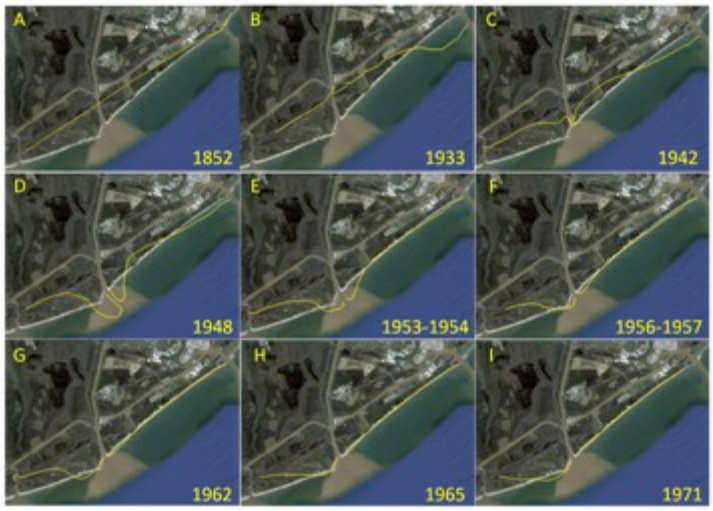

Figure 31: Historic changes in shoreline of the subaerial delta. Modified from Seelig and Sorenson (1973), and Google Earth. The 1852 shoreline (A) was prior to construction of the jetties at the old mouth.

The subaerial morphology of the delta has been well documented. Prior to the diversion of the river mouth, the river entered the Gulf of Mexico through what today is the Freeport Channel. The U.S. National Ocean Survey conducted a survey of the area in 1852 (Figure 31a). From this survey the Old Brazos Delta (OBD) largely resembled the present day configuration of Modern Brazos Delta (MBD), with an arcuate shape, and a

slight asymmetry favoring the down drift lobe. A mouth bar was present at the time of the survey. Jetties were constructed starting in 1881 and completed in 1899. These jetties caused the OBD to prograde approximately 1.6 km seaward and develop a strong asymmetry to the west (Figure 31b). This asymmetrical deposition resulted from the jetties interrupting the longshore currents, allowing for river derived sediment to rapidly accumulate down drift of the jetties (Seelig and Sorensen, 1973).

In 1929 the river was rerouted to its present location, and the MBD immediately began forming. While the MBD was prograding seaward, the OBD was retreating landward at approximately the same rate (Figure 31c). By 1948 the subaerial MBD had grown almost 2.5 km in less than 2 years, reaching its most seaward position. The subaerial delta exhibited a cuspate shape, and at this time the river mouth was deflected 45° eastward (Figure 31d). After 1948, the MBD began to retreat landward, and by 1953 the OBD shoreline had returned approximately to the same position it occupied in 1852 (Figure 31e and f). In 1961 Hurricane Carla made landfall approximately 100 km to the west of the MBD, as a category 4 hurricane as the second most intense hurricane to make landfall on the Texas coast, and ninth strongest to make landfall on the mainland US as of 2006 (Blake et al., 2007). The storm reworked sediment at the MBD, skewed the shape of the delta to west (Figures 31g-i), and initiated a westward migration of the delta (Seelig and Sorensen, 1973). Only a slight asymmetry of the subaerial delta is evident today compared to past configurations in the 1940s and 1950s.

The westward migration of the delta is best illustrated through the evolution of the nearby mouth of the San Bernard River (Figure 32). Located approximately 6 km southwest of the Brazos River mouth, the San Bernard River mouth maintained a funnel-shaped, slightly more open, down drift morphology (Figure 32b) from 1930 to 1967 (Kraus and Lin, 2002). From 1967 to 1983 the westward migration of the Brazos River delta began to encroach on the mouth of the San Bernard in the form of ridges, but without significant deflection of the mouth. Migration of the San Bernard mouth began in 1984 with the growth of a spit on the up drift flank, growth of the spit accelerated from 1989 to 1995 (Figure 32c), and by 2006 the mouth had closed (Figure 32f). In February of 2009 the mouth was reopened through dredging (Figure 32i), but by December 2012 the mouth had subsequently closed (www.sanbernardriver.com).

Figure 32: Imagery of the changes to the San Bernard River mouth over time. a) 2012 imagery showing San Bernard River mouth in relation to Brazos River mouth. The Intracoastal Water Way (ICWW) and beach ridges associated with the Brazos Delta (BDBR) highlighted. Below are images from the San Bernard River mouth in 1944 (b), 1995 (c), 2004 (d), 2005 (e), 2006 (f), 2008 (g), 2009 (h), 2010 (i), and 2011 (j). For reference the ICWW is labeled in (b) and the BDBR are labeled in (c) after forming post 1967. Images are from Google Earth.

4.3 Methods

Side scan sonar (SSS), and bathymetric data were collected on two cruises, February 10-13, 2011 and March 15-17, 2011, using a 200 kHz Teledyne Benthos® C3D-LPM High-Resolution Side-Scan Sonar Bathymetric System that collected SSS and bathymetric data concurrently. Survey transects were oriented parallel to the shore, spaced 100 m, constrained by the 3 and 10 m isobaths based on NOAA nautical chart 11321, and covering a total survey area of approximately 150 km^2, centered around the mouth of the river. The bathymetric data was corrected to mean low water (MLW) using NOAA tide station 8772447 located at the US Coast Guard station in Freeport, TX located approximately 10 km from the study area. Sub-bottom data was collected using an Edgetech® 216 Full Spectrum Sub-bottom CHIRP seismic sonar operating on frequencies between 2 and 16 kHz that was towed behind the vessel on June 6, 2011. Five sub-bottom survey transects were oriented shore-normal spaced throughout the SSS and bathymetry survey area. Two additional transects were oriented shore-oblique extending from the river mouth to the southwest and northeast respectively.

Sixty surface sediment grab samples were collected on July 8, 2011, and were analyzed in the lab for grain size distributions using a Malvern Mastersizer 2000® laser particle diffractometer. Sediment samples were homogenized, combined with a dispersant, and sonicated to prevent and break-up flocs prior to analysis. In total, the fraction of gravel (primarily small shells and shell fragments), sand, silt and clay were determined for each

sample, as well as the mean grain size, and other statistical properties could be determined as needed.

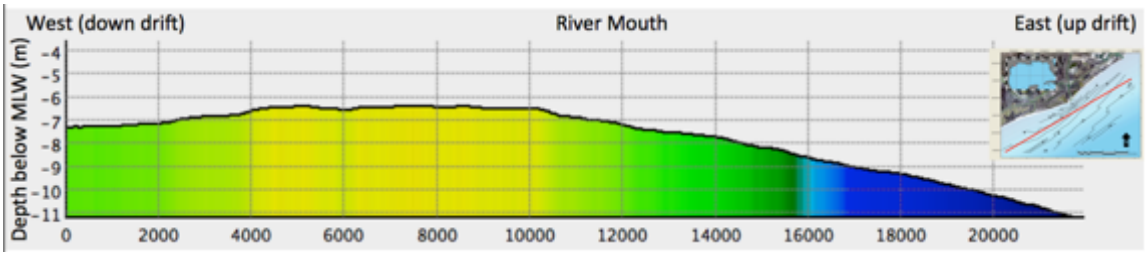

Figure 33: Bathymetric profile across the subaqueous delta from west to east showing the asymmetrical structure. Profile location shown in inset (red line), and approximate location of the river mouth is labeled.

4.4 Results

4.4.1 Bathymetry

The bathymetry of the subaqueous delta (Figure 30) shows a distinct asymmetry up drift (east) and down drift (west) of the river mouth as defined by the dominant longshore transport directions. On the up drift side, isobaths trend parallel to the shoreline and this area exhibits a relatively steep slope for the study site of ~1:625 or on average 0.09°. Down drift of the river mouth, water depths are shallower compared to the east, and only in depths less than 5 m do isobaths trend parallel to the shoreline. Water depths in this area of the subaqueous delta range from 2 m to 10 m below (MLW), with a slope of ~ 1:900 or on average ~0.07°. The bathymetric cross-section in Figure 33 highlights the difference in bathymetry between the up drift and down drift sides of the subaqueous delta.

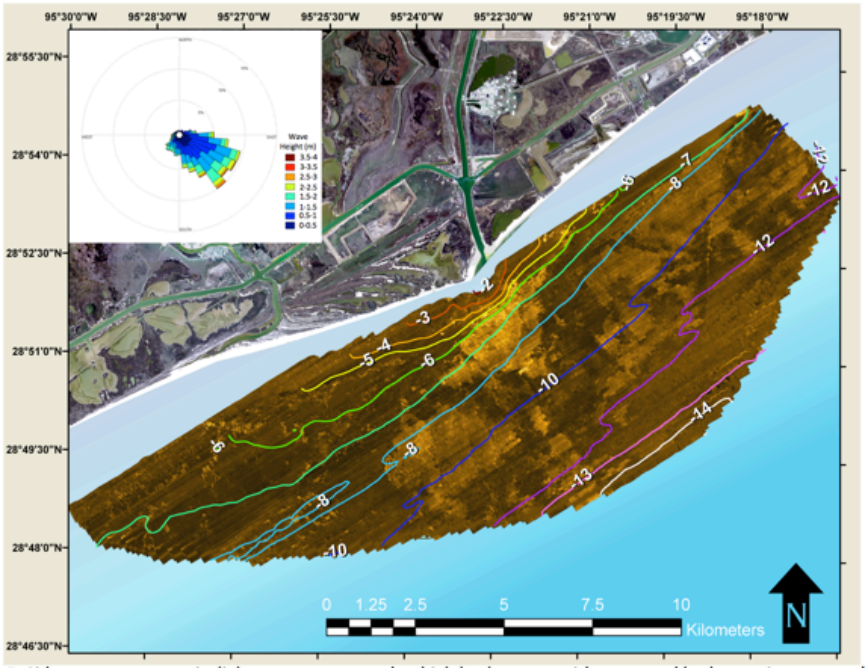

Figure 34: Side scan sonar mosaic. Light areas correspond to high backscatter, with measured bathymetric contours (m) overlain. Inset shows distribution of wave directions and associated wave heights in meters for the year 2009.

4.4.2 Side Scan Sonar

Results from the SSS showed a similar asymmetry as the bathymetry. The mosaic (Figure 34) shows three distinct backscatter characteristics, which are: 1) an area dominated by low backscatter (dark colors) with small isolated areas of high backscatter (light colors); 2) an area dominated by large, clearly defined high backscatter features; and 3) an area of moderate backscatter that lacks clearly defined features. It should be noted that the SSS backscatter data were normalized in order to enhance contrast over relatively small changes in backscatter. The low backscatter area is much smaller, wedge-shaped, and extends from the river mouth in a southwesterly orientation. Most of the mosaic is dominated by the high backscatter area, which is primarily seaward, and to

the east of the river mouth. Two large distinct high backscatter features were observed in the center of the survey area (Figure 35). The most dominant of these features (Feature A) is located directly seaward of the river mouth, encompassing an area of approximately 5 km^2, while the other feature (Feature B) is located approximately 5 km due south of the river mouth with an area of ~10 km^2. The western boundary of these features distinguishes the transition between the high backscatter and low backscatter areas of the mosaic. Figures 34 and 35 include the bathymetric contours to show the relationship between the features observed in the SSS mosaic and water depth. Figure 34 shows that the high backscatter observed in the eastern section of the study area is confined to water depths between 7 and 12 m. Feature A is bounded by the 5 m isobath directly adjacent to the river mouth, and the 6 m isobath on either side (Figure 35). This feature extends to just landward of the 10 m isobath. Feature B is located landward of the 8 m isobath and extends seaward of the 10 m isobath. The moderate backscatter area, the smallest of the three, is located southeast of the river mouth, near the seaward extent of the survey in water depths beyond 12 m.

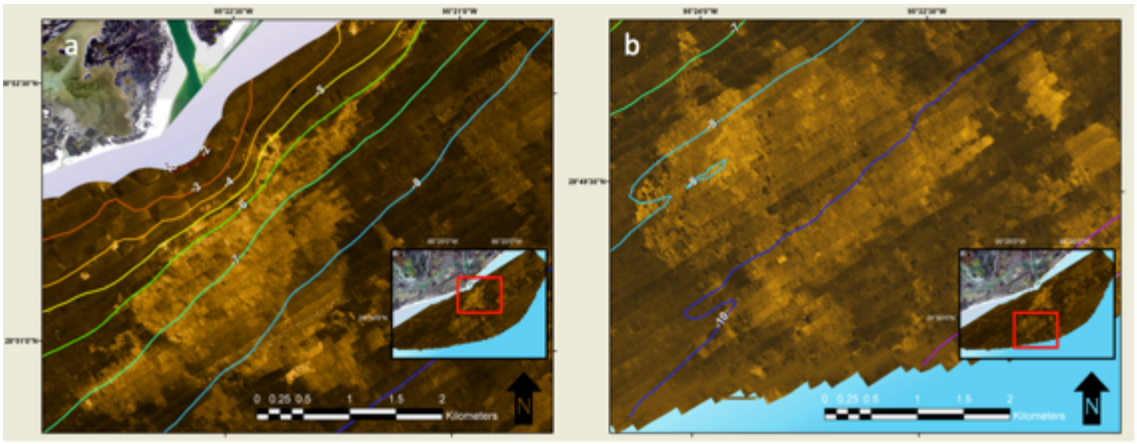

Figure 35: Zoomed image showing prominent high backscatter features from the side scan sonar mosaic. Feature A (left) and Feature B (right), with bathymetric contours.

4.4.3 Surface Sediment Characteristics

Figure 36 shows the results from the grain size analyses. This data includes results from the surface sediment grab samples as well as surface sediment from cores collected in September 2011 (Carlin and Dellapenna, in review). In Figure 36a the percentage of sand (> 63 μm) in the surface sediment are shown overlying the SSS mosaic, while Figure 36b shows the mean grain size of the surface sediment overlying the mosaic. Most of the sand is found down drift of the mouth in areas of low backscatter. Of the three areas where over 80% of the sediment consisted of sand, two are located down drift of the river mouth. With the one area up drift located within the nearshore zone. The smaller of the down drift depocenters is located approximately 2 km to the southwest of the river mouth, while the larger area is ~10 km to southwest of the river mouth near the seaward extent of the survey. These areas also correspond to areas where the mean grain size of the surface sediment is within the sand fraction. Outside of

these depocenters the sand content of the sediments decrease sharply to less than 20% in some areas. Most of the areas up drift of the river mouth are dominated by sediments consisting of 20% or less sand, with the exception of the nearshore sand depocenter mentioned above.

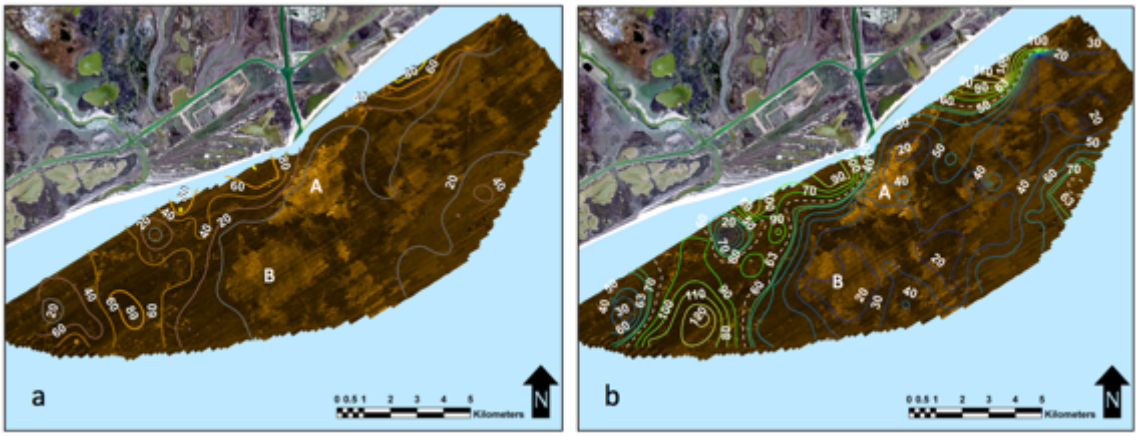

Figure 36: Side scan sonar mosaic with surface sediment characteristics. a) Percentage of coarse-grained (>63µm) surface sediment, and b) mean grain size (µm) of surface sediment. Dashed contour delineates sand/silt boundary (63µm) from Carlin (2013-this volume). Features A and B are labeled in white**.**

Another area with increased sand content (40% or more), and a sand-sized mean grain size, is found in the moderate backscatter area, a relatively flat, deep water (>12 m) area to the east of the river mouth. Most of the high backscatter areas, including Features A and B, correspond to mud (silts and clays) dominated sediment with a low (<20%) sand content. This suggests that the high backscatter muds are relict sediments that were exposed after having been buried and compacted, while low backscatter muddy-sand, and sand may be more recent, less-consolidated deposits. Furthermore, the surface sediment in the high backscatter areas is more homogenous in terms of percent sand and

mean size compared to the low backscatter and moderate backscatter areas, which exhibits significant changes in these properties over relatively short distances.

4.4.4 CHIRP

Throughout most of the survey area two prominent sub-bottom intervals are evident (Figure 37). The lowermost, shown in blue, is thickest, and consists of a series of parallel reflectors, relatively tightly spaced, oriented mostly horizontal. The surface of this sequence is a strong reflector oriented subparallel to the seabed. This sequence is interpreted as the relict clinoform, and sitting directly atop this reflector is the upper sequence in yellow, interpreted as the modern delta clinoform, deposited after human interventions to the system. The hard surface reflector between the two clinoforms may represent the seabed surface not only prior to the time of the river diversion, but also prior to the construction of the jetties at the old mouth in the 1890s. The modern clinoform consists of a series of seaward dipping, parallel to subparallel reflectors. The reflectors in the modern clinoform, up drift of the river mouth, exhibit a greater dip angle than those observed down drift of the river mouth, however the thickness of this modern clinoform is greater down drift of the river mouth. In addition, at the landward end of the lines, a pronounced offlap break is present, representing the steepest section of the lines. The offlap break also exhibits an asymmetry about the mouth, where it is much steeper on the up drift side. Figure 37b exhibits evidence of a past offlap break down drift of the river mouth that may correspond to an earlier stage in the MBD development. In some areas the record of the modern clinoform is obscured by shallow biogenic gas in

the sediments. The base of the sub-bottom record is the multiple shown as a solid red line, which obscures the data below.

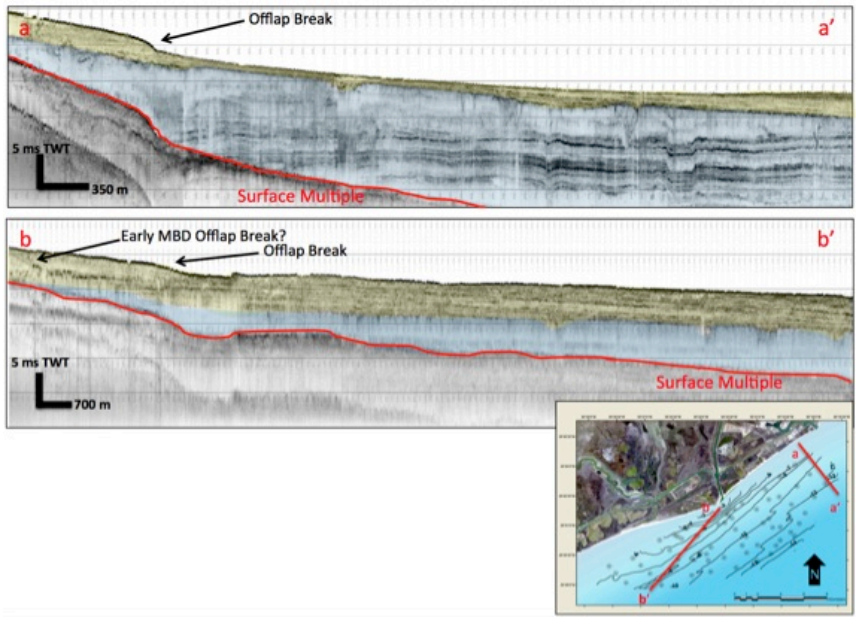

Figure 37: CHIRP profile from up drift of the river mouth (a), and down drift of the river mouth (b). Approximate location of the transects shown in the base map (right). Modern deltaic sequence is outlined in yellow; the relict shelf clinoform is in blue. Black arrows denote the offlap break, the area with the greatest slope, sometimes referred to as the rollover point, this represent the transition from topset to foreset. A potential early MBD offlap break is observed in the down drift profile (b). Red line indicates the surface multiple.

4.5 Discussion

Based on the changes to the subaerial delta as seen in the past shoreline configurations, three delta growth phases have been delineated: the Old Mouth, Modern Mouth, and Western Flank (Figure 38). Construction of jetties, completed in 1899, lead to progradation of OBD, and highlighted the first of the three subaerial delta growth phases. During this first phase the shoreline of the Old Mouth prograded over 1.5 km until the diversion of the river mouth. After the diversion, the Old Mouth began

retreating as the Modern Mouth began rapidly prograding. By 1952 the shoreline of the Modern Mouth prograded 3.5 km to its most seaward location, and then began retreating. For approximately a decade the entire subaerial delta retreated. In the early 1960's growth was reinitiated. Minimal growth was observed at the Modern Mouth, and by 1972 it had stabilized, and most of the growth occurred along the Western Flank of the modern delta, which prograded over 1 km during this period prograding across the mouth of the San Bernard River.

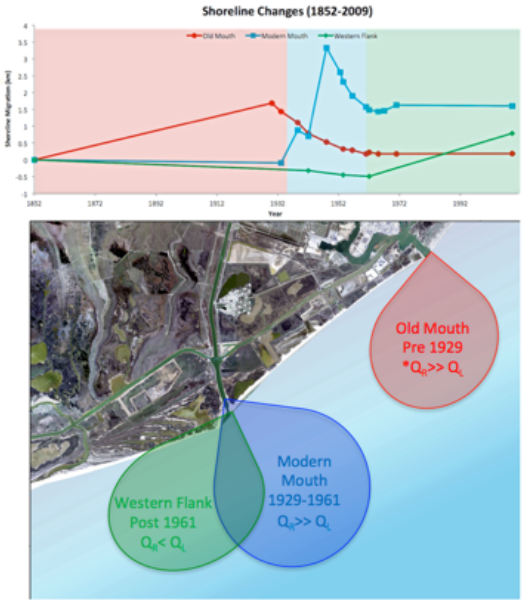

Figure 38: Shoreline changes from 1852 position for different sections of the delta. Background color indicates the times of specific subaerial delta growth phases, Old Mouth (red), Modern Mouth (blue), Western Flank (green). Bottom - Schematic showing the relative locations of the growth phases, the time period, and the suggested relationship at that time of sediment supply by the river (Q_R) and longshore drift (Q_L). *Old mouth growth was largely the result of jetty construction that was completed in 1899.

For the subaqueous delta, the general evolution can be seen as changes in bathymetry. Bathymetric data from this study collected in 2011 was compared to data sets from

surveys in 1938 and 1982. The results show that large portions of the study area have experienced net erosion of more than 4 meters in some places since 1938, nine years following the diversion, primarily located up drift of the river mouth (Figure 39). Down drift of the river mouth, the delta experienced net deposition of up to 2 meters since 1938. Slight accumulation since 1982 was observed in the moderate backscatter area seaward of the 12 m isobath. To this point, Carlin and Dellapenna (in review) observed evidence of erosion, and rapid changes in sediment accumulation rates within the sediments of the subaqueous delta. Data showed that sediment accumulated rapidly throughout the subaqueous delta after the river mouth was diverted, but rates have slowed over the past ~50 years, and most dramatically in the areas up drift of the river mouth where little sediment is presently accumulating.

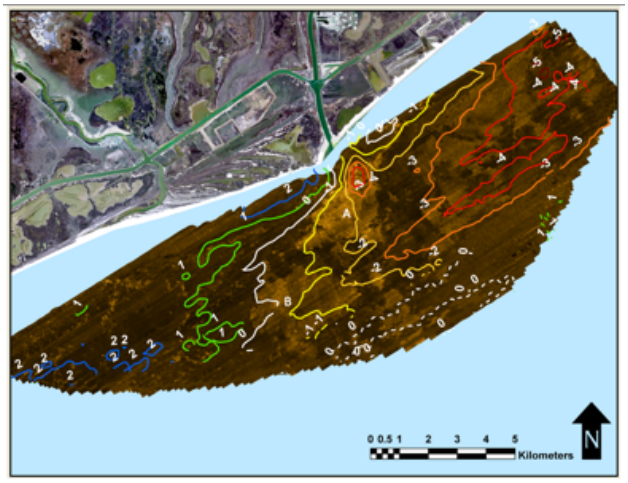

Figure 39: Side scan sonar mosaic with contours representing changes in bathymetry. Data is in meters and the difference between this survey and 1938 NOS Hydrographic Survey (solid lines) and a 1982 survey (dashed lines) courtesy of NOAA National Geophysical Data Center (right). Positive values equal net accumulation, no change is represented by the white lines. Features A and B are labeled in white.

From this data we conclude that the modern Brazos River subaqueous delta consists of two distinct lobes, the Eastern Lobe, which is erosion-dominated and accumulation limited, situated up drift of the present-day river mouth, and the actively accreting Western Lobe down drift of the present-day river mouth. As we will demonstrate, these lobes have been modulated both by human intervention within the watershed, the river and in the coastal zone as well as by a series of natural events, all resulting in feedback as the system continually shifts toward the maintenance of a dynamic equilibrium.

Figure 40: Side scan mosaic with the Eastern Lobe of the subaqueous delta outlined in red. Features A and B are labeled in white.

4.5.1 Eastern Lobe (Up drift)

The Eastern lobe of the subaqueous delta comprises most of the survey area (Figure 40). With an area in excess of 80 km^2, the Eastern Lobe is approximately two-thirds of the study area and includes both the high backscatter and moderate backscatter areas observed in the SSS mosaic. This lobe is delineated on its western boundary of the study

site by the 5 m and 6 m isobaths, the boundary of side scan Feature A, and the 20% sand content contour. Large areas of high backscatter, mud, and steeper slopes dominate this area. We conclude that Eastern Lobe of the subaqueous delta is comprised of the subaqueous components of the two early subaerial growth phases, the Old Mouth and Modern Mouth, although from the data it is difficult to distinguish the contribution from each individual phase.

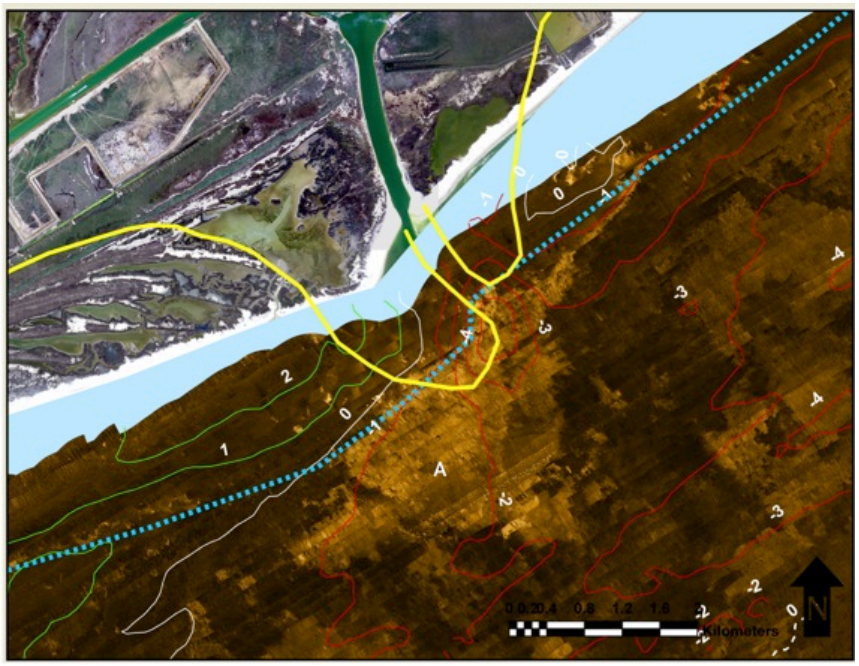

Figure 41: Side scan mosaic image of Feature A with 1948 shoreline (yellow solid line), change in bathymetry contours (green indicate net deposition, red indicate net erosion), and the location of the offlap break from the CHIRP data (blue dotted line). Feature A is labeled in white.

Although both growth phases contributed to this lobe, it is erosion that primarily characterizes this lobe. The Modern Mouth growth phase was the most rapid period of growth observed on the delta (Figure 38). This suggests that the sediment deposited was

highly unconsolidated and easily erodible, which is supported by the fact that the highest rate of shoreline retreat (~180 m/yr) was observed in this area in the late 1940's early 1950's. This can also be seen in the small area of elevated erosion (>4 m) near the Modern Mouth, associated with Feature A. Shown in Figure 41, this high-erosion area is located within Feature A, and at what would have been the river mouth in 1948. Currently this area is also bounded by the offlap break or roll over point on its landward side. The roll over point is considered the transition from the deltaic topset to foreset (Lobo et al., 2006; Walsh et al., 2004). Based the location of the 1948 shoreline, this point was likely located seaward of its present location, and has moved landward over time consistent with erosion. In addition, a sediment core collected from within this area of elevated erosion exhibited an unconformity approximately 10 cm from the surface suggesting an erosional surface, where the sediment below was interpreted from radioisotope data to be deposited prior to the early 1950's (Carlin and Dellapenna, in review).

The erosion in this area also explains the distinct, high backscatter features with sharp contacts that largely define the Eastern Lobe. Similar features have been described as mudflow gullies on the Mississippi River delta (Coleman, 1988), and silt flow gullies, highly textured seafloor, and collapse depressions on the Yellow River delta (Prior et al., 1986a; Prior et al., 1986b). With both of these deltas, these features were attributed to remobilization of sediment. Although the features in the Mississippi and Yellow River deltas were associated with a bathymetric expression, such an expression was not

apparent in our data. However, high backscatter features have been observed on the South Texas Continental Slope described as mass flow or slide deposits, potentially located downslope of an ancestral Brazos River delta deposited during a low stand in sea level when the river formed a shelf-edge delta (Rothwell et al., 1991). Similar to what we observed, these continental slope features have distinct boundaries, the upslope boundary is associated with a discrete isobath, and the feature exhibits little bathymetric expression. Rothwell et al. (1991) attributed the high backscatter associated with these features to uneven, hummocky small-scale topography, and sub-surfaces irregularities.

In addition, the CHIRP data from within the lobe shows evidence of erosion (Figure 37a). Sub-bottom data has proven effective at imaging clinoforms for a variety of deltaic systems including the Amazon (Nittrouer et al., 1986b), Atchafalaya (Allison and Neill, 2003; Neill and Allison, 2005), Po (Correggiari et al., 2005; Trincardi, 2004), Yangtze (Liu et al., 2006), and Yellow River deltas (Liu et al., 2004), as well as the Western Adriatic shelf (Cattaneo et al., 2007). However, unlike these prograding clinoforms, the modern clinoform in the Eastern Lobe thins in water depths between 4 and 8 m. Landward of the thinning, a relatively steep offlap break is observed, and the clinoform thickens at the seaward extent of the survey line. The changes in this relative thickness show that erosion of the modern clinoform has occurred in water depths between 4 and 8 m, above typical wave base, and suggests that sediment has been transported downslope, and deposited in deeper waters below typical wave base. This

deposition is located within the moderately high backscatter area, which has experienced relatively significant (~ 1 m) net deposition since the early 1980's.

Figure 42: Side scan mosaic with the Western Lobe of the subaqueous delta outlined in blue. Features A and B are labeled in white.

4.5.2 Western Lobe (Down drift)

The Western Lobe of the subaqueous delta occupies one-third of the study area, or approximately 40 km^2 (Figure 42). This lobe is principally defined by low backscatter, with the absence of the large distinct high backscatter features of the Eastern Lobe. Although small isolated areas of high backscatter are observed. Located directly seaward of the Modern river mouth, this lobe extends out in a southwestwardly direction. The slope of this lobe is gentler than the Eastern Lobe, with a maximum depth of approximately 10 m, compared to depths in excess of 14 m in the Eastern Lobe. Sand comprises a majority of the surface sediment in this lobe (Figure 36), and the majority of this lobe has shown net accretion, approximately 2 m in some areas (Figure 39). Carlin and Dellapenna (in review) found not only rapid long-term accumulation rates in this

area, but also rates decreased only slightly from ~2 cm/yr to ~1.5 cm/yr since the 1960s. This is in stark contrast to areas within the Eastern lobe, where accumulation dramatically slowed by an order of magnitude over the same time period. This Western Lobe represents the active subaqueous lobe, and also appears associated with the current growth phase, the Western Flank. The Western Lobe was likely activated in 1961 after Hurricane Carla shifted sediments to the west, down drift of the river mouth (Seelig and Sorensen, 1973).

The data shows that progradation of the subaqueous delta is confined to the Western lobe, and is occurring obliquely to the shore similar to the Atchafalaya delta in Louisiana (Allison and Neill, 2003). Since the 1960s accumulation has been estimated to be about 1.5 cm/yr (Carlin and Dellapenna, in review), which is comparable to the Po River Delta (Frignani and Langone, 1991), and the Atchafalaya (Allison and Neill, 2003). The CHIRP data also shows evidence of progradation as increased thickness of the modern clinoform (Figure 47b), with a relatively less steep offlap break overlying a relict offlap break suggested to be associated with the early stages of the MBD. Within the Western Lobe, the modern clinoform is generally around 4 m thick compared to the average 2 m thick within the Eastern Lobe. The thinning of the clinoform that was observed in the Eastern Lobe was not observed in this area.

Finally, the dominance of sand in the surface sediment in the area suggests that this lobe receives bedload from the river during flood events. The low gradient of the lobe,

allows for bottom-attached plumes from the river to transport bedload further offshore (Geyer et al., 2004). Noticeably there is an isolated sand depocenter (>80 % sand) in an area of the Western Lobe, 10 km from the river mouth (Figure 36a). This may represent a stranded sand deposit from the San Bernard River that has been cut off by accumulation of Brazos River sediment following the initiation of the Western Flank. Although in general the San Bernard water and sediment discharge is insignificant to the Brazos River, prior to the MBD impacting the mouth of the San Bernard, this river had an increased flow which could be significantly impacted by local storm events (Kraus and Lin, 2002). In addition the lack of large, well-defined high backscatter features in the Western Lobe, and the presence of small isolated high-backscatter features, may also be the result of Brazos River sediment covering relict San Bernard deposits.

Although it has been generally observed that increased coarse-grained sediment corresponds to high SSS backscatter, the opposite is observed within the Western Lobe. However two studies have shown an inverse relationship between grain-size and backscatter, one on the Eel Shelf (Borgeld et al., 1999), and the other from a Fjord in Quebec (Urgeles et al., 2002). On the Eel shelf low backscatter was associated with sandy inner-shelf areas of the prodelta terraces of the Eel and Mad Rivers. In the fjord in Quebec, a decrease in backscatter was observed following a flood event in which coarse sediment was deposited.

4.5.3 Fluvial Supply and Marine Processes

The changes observed over the history of the modern Brazos Delta can be attributed to changes in either the sediment supply from the river, or sediment reworking by marine processes. Shifts in the dominance between fluvial and marine forces have resulted from natural events and anthropogenic alterations to the system. The response of the delta is observed in the changes to both the subaerial and subaqueous delta, and preserved in the sediment record of the subaqueous delta within the two distinct lobes.

Alterations to the mouth began with the construction of the jetties in 1899. The jetties inhibited longshore transport down drift of the Old Mouth. As the ability to remove sediment from the subaqueous delta was reduced, the sediment supplied by the river initiated the Old Mouth growth phase of the subaerial delta down drift of the jetties (Figure 38). The shoreline prograded at a rate of approximately 55 m/yr, and continued until the river diversion in 1929. Sediment load data for the river date back to 1925, at this time the load was about 30 Mt/yr (Figure 43). We assume this value was established prior to the time of the Old Mouth progradation, the result of substantial increases in land clearing for agriculture, which began in the 19th Century and continued into the early 20th Century (Dunn and Raines, 2001). In spite of decades of this sediment load potentially being approximately three times the estimated load today, significant delta growth was only initiated after the construction of the jetties, highlighting the importance of disrupting the marine processes (i.e. longshore drift) to facilitate growth.

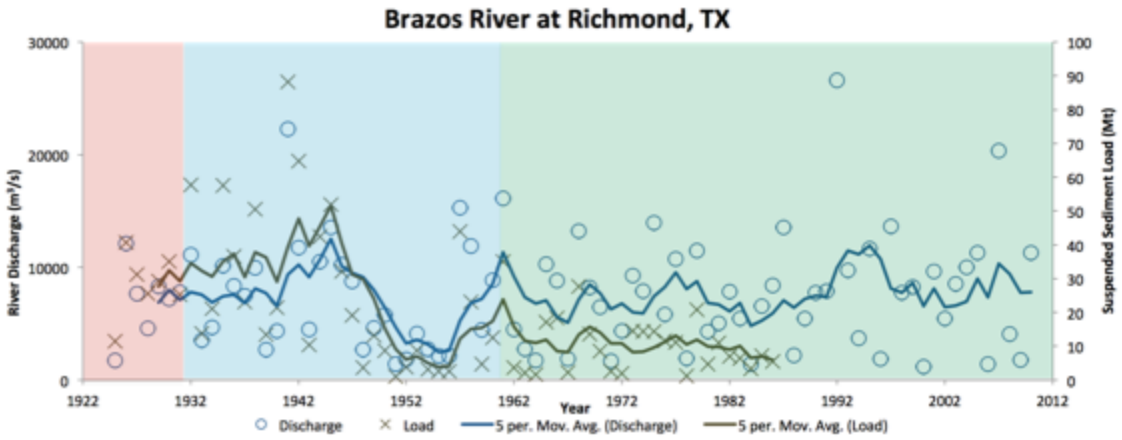

Figure 43: Average annual river discharge (blue circles) and annual sediment load (brown Xs) measured at the Richmond, TX gage station. Lines are 5 year running averages, and background colors are growth phases from Figure 38. Data courtesy of USGS and Texas Board of Water Engineers.

However, the most significant change to the river mouth was undoubtedly the diversion in 1929. When the river mouth was diverted, growth at the Old Mouth ceased, as it was no longer receiving input of fluvial sediment, and began retreating. This shoreline retreated at a rate of approximately 49 m/yr, almost the same rate as it had prograded. Cut-off from the fluvial supply of sediment, this shoreline returned to approximately the same position prior to construction of the jetties within a few decades. The retreat of the Old Mouth occurred during the Modern Mouth growth phase. At this time the Modern Mouth shoreline prograded at a rate 4 times that of the Old Mouth, 228 m/yr. Through the 1930s the sediment load in the river remained near the 30 Mt/yr level, but increased in the 1940s to 40 – 50 Mt/yr. However, this increase in sediment load would not solely account for the four-fold increase in progradation. A significant portion of the sediment must have been sourced from the now eroding Old Mouth shoreline, and Eastern Lobe of

the subaqueous delta to facilitate this rapid growth rate. At the peak of progradation of the MBD the delta had developed a cuspate shape and the river mouth had been deflected up drift. A similar sequence was observed on the Simeto River delta in eastern Sicily, where during the prograding phase of the delta, the river mouth also developed a cuspate shape and was deflected up drift, and during the receding phase the mouth become more arcuate and deflected down drift (Longhitano and Colella, 2007). These changes were also attributed to changes in the relationship between the sediment supplied by the river and the amount reworked through oceanographic processes. This period following the diversion of the Brazos River mouth, during the Modern Mouth growth phase, was likely a time when sediment supply outpaced marine processes, as the supply of sediment was a combination of the elevated sediment load of the river, and erosion up drift of the new mouth leading to the unprecedented growth.

In the late 1940s the sediment load dropped to below 10 Mt/yr (Figure 43) and all areas of the delta were retreating. The Modern Mouth shoreline retreated at a rate upwards of 180 m/yr, twice as fast as the retreat of Old Mouth Lobe. In addition to this reduction in sediment load, the average annual discharge of the river was also dramatically reduced. This reduction in discharge and sediment load resulted from a combination of events, both natural and anthropogenic. Changes in agricultural practices following the Dust Bowl in the 1930s reduced sediment availability (Seelig and Sorensen, 1973). Other changes in agricultural practices include a reduction in non-hay producing cropland, and the conversion of cropland to pastureland, both of which reduce the erosion potential of

the land in the watershed. Croplands are plowed each season, and are vastly more vulnerable to erosion than pasture land, which is unplowed. This occurred gradually over the 20th Century (Dunn and Raines, 2001). Finally, dam construction, which decreases sediment discharge (Milliman and Syvitski, 1992), began in 1941 at Possum Kingdom Lake over 500 km inland of the river mouth, and then in 1951 with Lake Whitney 400 km inland, the two largest impounds within the drainage basin, and both are located on the main stem of the river (Dunn and Raines, 2001).

Although these factors contributed to a reduction in sediment load of the river, it is expected that a gradual decrease in sediment load over time would have been observed. From Figure 43, there is a near instantaneous reduction in the sediment load of the river, from around 50 Mt/yr to less than 10 Mt/yr, in only a couple of years. Furthermore, this reduction in sediment load is coupled with an equally dramatic reduction in discharge of the river. These rapid changes to the hydrograph of the river resulted from a prolonged drought that occurred from 1948 – 1957 (Norwine and Bingham, 1985) termed "The Little Dust Bowl" (Opie, 1989). As the sediment load delivered to the delta was reduced during the drought, longshore transport became dominant in reworking and removing sediment, initiating delta-wide retreat. As the drought relaxed toward the end of the 1950s, the river discharge returned to pre-drought levels, the sediment load also increased, but remained about 20% of the pre-drought level at 10 Mt/yr. This prolonged reduction in load likely reflects the changes in agricultural practices.

After this time the sediment load stabilized to rate of between 10 and 16 Mt/yr, approximately half of the pre-1940s rate, and initiated progradation in the Western Flank at a rate of about 27 m/yr, approximately half of the Old Mouth progradation rate. At this time the delta transitioned back into a marine dominated phase. This is made clear by the effect Hurricane Carla in 1961 had on the delta. A Category 4 Hurricane, this storm made landfall approximately 100 km to the west as the 9th strongest storm to make landfall on the United States (Blake et al., 2007). This storm, which generated >3 m storm surge near the delta, shifted sediment westward (Seelig and Sorensen, 1973), initiating the growth in the Western Flank of the delta. Since this storm, growth has only been observed in this area, and results from this study suggest a predominantly westward dispersal of marine sediments. Westward migration of sediment is confirmed by the closing of the mouth of the nearby San Bernard River (Figure 32) that was first impacted starting in 1967 after the initiation of The Western Flank. The growth of the Western Flank has lead to a more symmetric subaerial delta, which is predicted by models given the reduction in fluvial sediment supply (Figure 43), and low angle dominant wave direction (Ashton and Giosan, 2011). These trends indicate that presently, longshore transport dominates, moving sediments down drift faster than what the river can supply. Furthermore, Carlin and Dellapenna (in review) suggests that as much as 90% of the sediment load of the river is bypassing the study area, supporting the idea of a marine dispersal dominated system over the past ~ 50 years.

4.6 Conclusion

The Brazos River delta represents a modern delta, one that is influenced by both natural and anthropogenic forces. As a result, the delta has undergone dramatic changes over short periods of time. Rapid shoreline transgressions and regressions were the results of human activity within the watershed, to the coastline directly, and natural events including floods, droughts, and hurricanes. This study showed that the dynamic evolution of this modern delta is not only chronicled in historical photographs and imagery, but also preserved in the subaqueous delta sediments. These results indicate that changes, natural or anthropogenic, in the balance in the sediment supplied by the river, and the sediment remobilized by marine processes, can result in dramatic changes to both the subaerial and subaqueous delta. Changes in this balance have lead to three growth phases of the subaerial delta. Growth of the Old Mouth occurred after the completion of the jetties in 1899, which interrupted longshore drift and facilitated accumulation. The Modern Mouth phase occurred after the diversion of the mouth, as elevated sediment loads from the river coupled with sediment supplied from the retreating Old Mouth facilitated the fastest growth of the delta. During drought conditions in the 1950s the Modern Mouth retreated, and Hurricane Carla in 1961 redistributed sediments westward, and initiated growth in the Western Flank of the Delta. These three phases created two distinct subaqueous delta lobes; the Eastern Lobe characterized by erosion of the Old and Modern Mouth growth phases, and the Western Lobe that is actively prograding and accumulating sediment. The current growth of the delta has resulted from a reduced sediment load of the river, initiated by the drought and

maintained by changes in agricultural practices, that has resulted in a system that is dominated by marine dispersal of fluvial sediments. Presently, the majority of the sediment load of the river may actually bypass the subaqueous delta at the mouth and be transported along the shelf, or across the shelf into deeper waters.

5 CONCLUSION

The conclusions of this work include that for the lower Brazos River a marine water intrusion in the form of a salt wedge is present at river discharges above mean discharge. Potentially as much as 80% of the time a salt wedge may be present in the lower river extending at least as far at 15 km from the mouth. While the salt wedge is present in the lower river, sediment is trapped forming an ephemeral mud layer. When discharge exceeds a threshold, for this study it was determined to be approximately 300 m^3/s, the salt wedge is pushed seaward of the river mouth, and sediment may be exported to the coastal ocean via a buoyant plume. During these export events, the ephemeral mud layer may be remobilized thereby increasing the sediment concentration beyond what the rating curve may estimate. During prolonged floods, the entire ephemeral mud layer may be exported.

This shows that sediment export to the coastal ocean and the subaqueous delta is episodic, occurring on event-scales. The sediments of the proximal subaqueous delta confirm this mechanism. Brazos River sediment can be distinguished from background Gulf of Mexico sediment by their color, internal bedding, bulk density, and relative calcium abundance. The data from the subaqueous delta show that the area proximal to the river mouth exhibits the attributes typical of a delta foreset region, with non steady-state sedimentation, relatively high sedimentation rates, physical stratification within the sediment record, and an over lack of bioturbation. Furthermore evidence of erosion, and changes in the primary depocenters were also observed, as presently most of the

sediment from the river is dispersed westward from the river mouth, and as much a 92% of the sediment may be bypassing the study area.

The westward dispersal of sediment and the lack of a majority of fluvial sediment being retained within the area proximal to the mouth suggests that currently the system is dominated by marine processes dispersing sediment. Over the history of the delta the balance between fluvial supply and marine dispersal of sediment has fluctuated, leading to dramatic changes in the delta. A period of rapid growth of the delta followed the construction of jetties at the OBD mouth that interrupted longshore transport. The diversion of the river mouth in 1929 caused rapid growth of the MBD, while initiating retreat in the MBD as it was cut off from the supply of sediment. Drought in the 1950s, changes in agricultural practices in the watershed, and construction of dams reduced the sediment load to the delta and initiated retreat until the new equilibrium was reached.

This dissertation utilized the lower Brazos River and proximal Gulf of Mexico to investigate the transport of terrestrial material to the coastal ocean, the fate this material in the coastal ocean, and the response of a delta to natural and anthropogenic alterations to the ecosystem. From this work, a better understanding of the sediment transport mechanisms of the Brazos River, and sediment preservation mechanisms of the Brazos Subaqueous Delta was achieved. These results may be applied to better understand similar systems throughout the world as increasingly more costal areas are impacted by human activities, and global climate change.

REFERENCES

Adams, C.E., Swift, D.J.P., Coleman, J.M., 1987. Bottom Currents And Fluviomarine Sedimentation On The Mississippi Prodelta Shelf - February-May 1984. Journal of Geophysical Research-Oceans 92, 14595-14609.

Allison, M.A., Kineke, G.C., Gordon, E.S., Goni, M.A., 2000. Development and reworking of a seasonal flood deposit on the inner continental shelf off the Atchafalaya River. Continental Shelf Research 20, 2267-2294.

Allison, M.A., Neill, C.F., 2003. Development of a Modern Subaqueous Mud Delta on the Atchafalaya Shelf, Louisiana, in: Scott, E.D., Bouma, A.H., Bryant, W.R. (Eds.), Siltstones, Mudstones, and Shales: Depositional Processes and Characteristics. SEPM (Society for Sedimentary Geology) and Gulf Coast Association of Geological Societies (GCAGS), pp. 23-34.

Ashton, A.D., Giosan, L., 2011. Wave-angle control of delta evolution. Geophysical Research Letters 38, 6.

Balsam, W.L., Beeson, J.P., 2003. Sea-floor sediment distribution in the Gulf of Mexico. Deep Sea Research Part I: Oceanographic Research Papers 50, 1421-1444.

Bentley, S.J., Nittrouer, C.A., 1999. Physical and biological influences on the formation of sedimentary fabric in an oxygen-restricted depositional environment; Eckernforde Bay, southwestern Baltic Sea. Palaios 14, 585-600.

Bhattacharya, J.P., Giosan, L., 2003. Wave-influenced deltas: geomorphological implications for facies reconstruction. Sedimentology 50, 187-210.

Bianchi, T.S., Allison, M.A., 2009. Large-river delta-front estuaries as natural "recorders" of global environmental change. Proceedings of the National Academy of Sciences of the United States of America 106, 8085-8092.

Blake, E.S., Rappaport, E.N., Landsea, C.W., 2007. The Deadliest, Costliest, and Most Intense United States Tropical Cyclones From 1851 to 2006 (And Other Frequently Requested Hurricane Facts), in: Center, N.H. (Ed.). National Weather Service, Miami, FL.

Borgeld, J.C., Hughes Clarke, J.E., Goff, J.A., Mayer, L.A., Curtis, J.A., 1999. Acoustic backscatter of the 1995 flood deposit on the Eel shelf. Marine Geology 154, 197-210.

Byrne, J.R., 1975. Holocene depositional history of Lavaca Bay, Central Texas Gulf Coast. University of Texas, Austin, Austin.

Cattaneo, A., Trincardi, F., Asioli, A., Correggiari, A., 2007. The Western Adriatic shelf clinoform: energy-limited bottomset. Continental Shelf Research 27, 506-525.

Coleman, J.M., 1982. Deltas: Processes of Deposition and Models for Exploration. International Human Resources Developement Corporation, Boston.

Coleman, J.M., 1988. Dynamic Changes And Processes In The Mississippi River Delta. Geological Society of America Bulletin 100, 999-1015.

Corbett, D.R., Mckee, B., Allison, M., 2006. Nature of decadal-scale sediment accumulation on the western shelf of the Mississippi River delta. Continental Shelf Research 26, 2125-2140.

Correggiari, A., Cattaneo, A., Trincardi, F., 2005. The modern Po Delta system: Lobe switching and asymmetric prodelta growth. Marine Geology 222, 49-74.

Crockett, J., Nittrouer, C., 2004. The sandy inner shelf as a repository for muddy sediment: an example from Northern California. Continental Shelf Research 24, 55-73.

Croudace, I.W., Rindby, A., Rothwell, R.G., 2006. ITRAX: description and evaluation of a new multi-function X-ray core scanner. SPECIAL PUBLICATION-GEOLOGICAL SOCIETY OF LONDON 267, 51.

Curray, J.R., 1960. Sediments and History of Holocene Transgression, Contiental Shelf, Northwest Gulf of Mexico, in: Shepard, F.P., Phleger, F.B., Van Andel, T.H. (Eds.), Recent Sediments, Northwest Gulf of Mexico: ASymposium Summarizing the Results of Work Carried On in Project 51 of the American Petroleum Institute 1951-1958. The American Association of Petroleum Geologists, Tulsa, Oklahoma, U.S.A., pp. 221-266.

Dalrymple, R., Zaitlin, B., Boyd, R., 1992. A conceptual model of estuarine sedimentation. Journal of Sedimentary Petrology 62, 116.

DeMaster, D.J., McKee, B.A., Nittrouer, C.A., Jiangchu, Q., Guodong, C., 1985. Rates of sediment accumulation and particle reworking based on radiochemical measurements from continental shelf deposits in the East China Sea. Continental Shelf Research 4, 143-158.

Dukat, D.A., Kuehl, S.A., 1995. Non-steady-state 210Pb flux and the use of 228Ra/226Ra as a geochronometer on the Amazon continental shelf. Marine Geology 125, 329-350.

Dunn, D.D., Raines, T.H., 2001. Indications and Potential Sources of Change in Sand Transport in the Brazos River, Texas. U.S. Geological Survey.

Dyer, K., 1994. Estuarine sediment transport and deposition, in: Pye, K. (Ed.), Sediment transport and depositional processes. Blackwell Scientific Publishing, Boston, pp. 193-218.

Farnsworth, K.L., Milliman, J.D., 2003. Effects of climatic and anthropogenic change on small mountainous rivers: the Salinas River example. Global and Planetary Change 39, 53-64.

Fraticelli, C.M., 2006. Climate Forcing in a Wave-Dominated Delta: The Effects of Drought–Flood Cycles on Delta Progradation. Journal of Sedimentary Research 76, 1067-1076.

Frignani, M., Langone, L., 1991. Accumulation Rates And Cs-137 Distribution In Sediments Off The Po River Delta And The Emilia-Romagna Coast (Northwestern Adriatic Sea, Italy). Continental Shelf Research 11, 525-542.

Frignani, M., Langone, L., Ravaioli, M., Sorgente, D., Alvisi, F., Albertazzi, S., 2005. Fine-sediment mass balance in the western Adriatic continental shelf over a century time scale. Marine Geology 222, 113-133.

Galler, J.J., Allison, M.A., 2008. Estuarine controls on fine-grained sediment storage in the Lower Mississippi and Atchafalaya Rivers. Geological Society of America Bulletin 120, 386-398.

Geyer, W.R., 1993. The importance of suppression of turbulence by stratification on the estuarine turbidity maximum. Estuaries and Coasts 16, 113-125.

Geyer, W.R., Hill, P.S., Kineke, G.C., 2004. The transport, transformation and dispersal of sediment by buoyant coastal flows. Continental Shelf Research 24, 927-949.

Geyer, W.R., Kineke, G.C., 1995. Observations Of Currents And Water Properties In The Amazon Frontal Zone. Journal of Geophysical Research-Oceans 100, 2321-2339.

Geyer, W.R., Woodruff, J.D., Traykovski, P., 2001. Sediment transport and trapping in the Hudson River estuary. Estuaries 24, 670-679.

Gibbs, R.J., 1970. Circulation in Amazon-River Estuary and Adjacent Atlantic-Ocean. Journal of Marine Research 28, 113-&.

Goodbred, S.L., Kuehl, S.A., Steckler, M.S., Sarker, M.H., 2003. Controls on facies distribution and stratigraphic preservation in the Ganges-Brahmaputra delta sequence. Sedimentary Geology 155, 301-316.

Grant, W.D., Madsen, O.S., 1986. The continental-shelf bottom boundary layer. Annual Review of Fluid Mechanics 18, 265-305.

Islam, M.R., Begum, S.F., Yamaguchi, Y., Ogawa, K., 2002. Distribution of suspended sediment in the coastal sea off the Ganges-Brahmaputra River mouth: observation from TM data. Journal of Marine Systems 32, 307-321.

Keeney-Kennicutt, W.L., Presley, B.J., 1986. The geochemistry of trace metals in the Brazos River estuary. Estuarine, Coastal and Shelf Science 22, 459-477.

Kim, W., Mohrig, D., Twilley, R., Paola, C., Parker, G., 2009. Is it feasible to build new land in the Mississippi River Delta? EOS, Transactions American Geophysical Union 90, 373-374.

Kineke, G.C., Sternberg, R.W., Trowbridge, J.H., Geyer, W.R., 1996. Fluid-mud processes on the Amazon continental shelf. Continental Shelf Research 16, 667-696.

Kolker, A.S., Allison, M.A., Hameed, S., 2011. An evaluation of subsidence rates and sea-level variability in the northern Gulf of Mexico. Geophysical Research Letters 38, L21404.

Kraus, N.C., Lin, L., 2002. Coastal Processes Study of San Bernard River Mouth, Texas: Stability and Maintenance of Mouth. DTIC Document.

Krishnaswamy, S., Lal, D., Martin, J., Meybeck, M., 1971. Geochronology of lake sediments. Earth and Planetary Science Letters 11, 407-414.

Kuehl, S.A., Brunskill, G.J., Burns, K., Fugate, D., Kniskern, T., Meneghini, L., 2004. Nature of sediment dispersal off the Sepik River, Papua New Guinea: preliminary sediment budget and implications for margin processes. Continental Shelf Research 24, 2417-2429.

Kuehl, S.A., DeMaster, D.J., Nittrouer, C.A., 1986. Nature of sediment accumulation on the Amazon continental shelf. Continental Shelf Research 6, 209-225.

Kuehl, S.A., Hariu, T.M., Moore, W.S., 1989. Shelf sedimentation off the Ganges-Brahmaputra river system: Evidence for sediment bypassing to the Bengal fan. Geology 17, 1132-1135.

Kuehl, S.A., Levy, B.M., Moore, W.S., Allison, M.A., 1997. Subaqueous delta of the Ganges-Brahmaputra river system. Marine Geology 144, 81-96.

Kuehl, S.A., Pacioni, T.D., Rine, J.M., 1995. Seabed dynamics of the inner Amazon continental shelf: temporal and spatial variability of surficial strata. Marine Geology 125, 283-302.

Liu, J.P., Li, A.C., Xu, K.H., Veiozzi, D.M., Yang, Z.S., Milliman, J.D., DeMaster, D., 2006. Sedimentary features of the Yangtze River-derived along-shelf clinoform deposit in the East China Sea. Continental Shelf Research 26, 2141-2156.

Liu, J.P., Milliman, J.D., Gao, S., Cheng, P., 2004. Holocene development of the Yellow River subaqueous delta, North Yellow Sea. Marine Geology 209, 45-67.

Lobo, F.J., Fernandez-Salas, L.M., Moreno, I., Sanz, J.L., Maldonado, A., 2006. The sea-floor morphology of a Mediterranean shelf fed by small rivers, northern Alboran Sea margin. Continental Shelf Research 26, 2607-2628.

Longhitano, S., Colella, A., 2007. Geomorphology, sedimentology and recent evolution of the anthropogenically modified Simeto River delta system (eastern Sicily, Italy). Sedimentary Geology 194, 195-221.

McGowen, J., Garner, L., Wilkinson, B.H., 1977. The Gulf shoreline of Texas: processes, characteristics, and factors in use.

McKee, B.A., Nittrouer, C.A., DeMaster, D.J., 1983. Concepts of sediment deposition and accumulation applied to the continental shelf near the mouth of the Yangtze River. Geology 11, 631-633.

Milliman, J.D., Meade, R.H., 1983. World-wide delivery of river sediment to the oceans. The Journal of Geology, 1-21.

Milliman, J.D., Syvitski, J.P.M., 1992. Geomorphic Tectonic Control of Sediment Discharge to the Ocean - the Importance of Small Mountainous Rivers. Journal of Geology 100, 525-544.

Neill, C.F., Allison, M.A., 2005. Subaqueous deltaic formation on the Atchafalaya Shelf, Louisiana. Marine Geology 214, 411-430.

Nielsen-Gammon, J.W., 2012. The 2011 Texas Drought. Texas Water Journal 3.

Nittrouer, C., DeMaster, D., McKee, B., 1984a. Fine-scale stratigraphy in proximal and distal deposits of sediment dispersal systems in the East China Sea. Marine Geology 61, 13-24.

Nittrouer, C., DeMaster, D., McKee, B., Cutshall, N., Larsen, I., 1984b. The effect of sediment mixing on Pb-210 accumulation rates for the Washington continental shelf. Marine Geology 54, 201-221.

Nittrouer, C.A., Curtin, T.B., Demaster, D.J., 1986a. Concentration and Flux of Suspended Sediment on the Amazon Continental-Shelf. Continental Shelf Research 6, 151-174.

Nittrouer, C.A., Kuehl, S.A., Demaster, D.J., Kowsmann, R.O., 1986b. The Deltaic Nature Of Amazon Shelf Sedimentation. Geological Society of America Bulletin 97, 444-458.

Nittrouer, C.A., Kuehl, S.A., Figueiredo, A.G., Allison, M.A., Sommerfield, C.K., Rine, J.M., Faria, L.E.C., Silveira, O.M., 1996. The geological record preserved by Amazon shelf sedimentation. Continental Shelf Research 16, 817-841.

Nittrouer, C.A., Sternberg, R.W., Carpenter, R., Bennett, J.T., 1979. Use Of Pb-210 Geochronology As A Sedimentological Tool - Application To The Washington Continental-Shelf. Marine Geology 31, 297-316.

Norwine, J., Bingham, R., 1985. Frequency and severity of droughts in south Texas: 1900-1983, in: Brown, R.D. (Ed.), Livestock and Wildlife Management During Drought. Caeser Kleberg Wildlife Research Institute, Kingsville, Texas.

Nowlin Jr, W.D., Jochens, A.E., DiMarco, S.F., Reid, R.O., Howard, M.K., 2005. Low-Frequency Circulation Over the Texas-Louisiana Continental Shelf, in: Sturges, W., Lugo-Fernández, A. (Eds.), Circulation in the Gulf of Mexico: observations and models: Geophysical monograph series. American Geophysical Union, Washington D.C., pp. 219-240.

Opie, J., 1989. 100 Years Of Climate Risk Assessment On The High-Plains - Which Farm Paradigm Does Irrigation Serve. Agricultural History 63, 243-269.

Palinkas, C., Nittrouer, C., 2006. Clinoform sedimentation along the Apennine shelf, Adriatic Sea. Marine Geology 234, 245-260.

Palinkas, C., Nittrouer, C., 2007. Modern sediment accumulation on the Po shelf, Adriatic Sea. Continental Shelf Research 27, 489-505.

Palinkas, C., Nittrouer, C., Walsh, J., 2006. Inner-shelf sedimentation in the Gulf of Papua, New Guinea: A mud-rich shallow shelf setting. Journal of Coastal Research, 760-772.

Postma, H., 1967. Sediment Transport and Sedimentation in the Estuarine Environment. Estuaries 83, 158.

Prior, D.B., Yang, Z.S., Bornhold, B.D., Keller, G.H., Lin, Z.H., Wiseman, W.J., Wright, L.D., Lin, T.C., 1986a. The Subaqueous Delta Of The Modern Huanghe (Yellow-River). Geo-Marine Letters 6, 67-75.

Prior, D.B., Yang, Z.S., Bornhold, B.D., Keller, G.H., Lu, N.Z., Wiseman, W.J., Wright, L.D., Zhang, J., 1986b. Active Slope Failure, Sediment Collapse, And Silt Flows On The Modern Subaqueous Huanghe (Yellow-River) Delta. Geo-Marine Letters 6, 85-95.

Rodriguez, A.B., Hamilton, M.D., Anderson, J.B., 2000. Facies and Evolution of the Modern Brazos Delta, Texas: Wave vs Flood Influence. Journal of Sedimentary Research 70, 283-295.

Rothwell, R., Kenyon, N.H., McGregor, B., 1991. Sedimentary features of the South Texas continental slope as revealed by side-scan sonar and high-resolution seismic data. American Association of Petroleum Geologists Bulletin 75, 298-312.

Rothwell, R.G., Rack, F.R., 2006. New techniques in sediment core analysis: an introduction. Geological Society, London, Special Publications 267, 1-29.

Santschi, P.H., Guo, L.D., Asbill, S., Allison, M., Kepple, A.B., Wen, L.S., 2001. Accumulation rates and sources of sediments and organic carbon on the Palos Verdes shelf based on radioisotopic tracers (Cs-137, Pu-239,Pu-240, Pb-210, Th-234, U-238 and C-14). Marine Chemistry 73, 125-152.

Seelig, W.N., Sorensen, R.M., 1973. Investigation of Shoreline Changes at Sargent Beach, Texas, TAMU-SG-73-212 ed. Texas A&M University Sea Grant p. 153.

Simeoni, U., Corbau, C., 2009. A review of the Delta Po evolution (Italy) related to climatic changes and human impacts. Geomorphology 107, 64-71.

Simonsson, M., Hillier, S., Öborn, I., 2009. Changes in clay minerals and potassium fixation capacity as a result of release and fixation of potassium in long-term field experiments. Geoderma 151, 109-120.

Sionneau, T., Bout-Roumazeilles, V., Biscaye, P.E., Van Vliet-Lanoe, B., Bory, A., 2008. Clay mineral distributions in and around the Mississippi River watershed and Northern Gulf of Mexico: sources and transport patterns. Quaternary Science Reviews 27, 1740-1751.

Siringan, F.P., Anderson, J.B., 1993. Seismic Facies, Architecture, and Evolution of the Bolivar Roads Tidal Inlet Delta Complex, East Texas Gulf-Coast. Journal of Sedimentary Petrology 63, 794-808.

Soileau, C.W., Garrett, B.J., Thibodeaux, B.J., 1989. Drought Induced Saltwater Intrusion on the Mississippi River.

Sommerfield, C.K., Nittrouer, C.A., 1999. Modern accumulation rates and a sediment budget for the Eel shelf: a flood-dominated depositional environment. Marine Geology 154, 227-241.

Strauss, J., Grossman, E.L., Carlin, J.A., Dellapenna, T.M., 2012. 100 Years of benthic foraminiferal history on the inner Texas shelf inferred from fauna and stable isotopes: Preliminary results from two cores. Continental Shelf Research.

Sylvia, D.A., Galloway, W.E., 2006. Morphology and stratigraphy of the late Quaternary lower Brazos valley: Implications for paleo-climate, discharge and sediment delivery. Sedimentary Geology 190, 159-175.

Syvitski, J., 2008. Deltas at risk. Sustainability Science 3, 23-32.

Syvitski, J.P., Morehead, M.D., 1999. Estimating river-sediment discharge to the ocean: application to the Eel margin, northern California. Marine Geology 154, 13-28.

Syvitski, J.P., Morehead, M.D., Bahr, D.B., Mulder, T., 2000. Estimating fluvial sediment transport: The rating parameters. Water Resources Research 36, 2747-2760.

Syvitski, J.P.M., Kettner, A., 2011. Sediment flux and the Anthropocene. Philosophical Transactions of the Royal Society a-Mathematical Physical and Engineering Sciences 369, 957-975.

Syvitski, J.P.M., Saito, Y., 2007. Morphodynamics of deltas under the influence of humans. Global and Planetary Change 57, 261-282.

Trincardi, F., Antonio Cattaneo, and Annamaria Correggiari, 2004. Mediterranean Prodelta Systems: Natural Evolution and Human Impact Investigated by EURODELTA. Oceanography 17, 34-45.

Urgeles, R., Locat, J., Schmitt, T., Hughes Clarke, J.E., 2002. The July 1996 flood deposit in the Saguenay Fjord, Quebec, Canada: implications for sources of spatial and temporal backscatter variations. Marine Geology 184, 41-60.

Walsh, J.P., Nittrouer, C.A., 2009. Understanding fine-grained river-sediment dispersal on continental margins. Marine Geology 263, 34-45.

Walsh, J.P., Nittrouer, C.A., Palinkas, C.M., Ogston, A.S., Sternberg, R.W., Brunskill, G.J., 2004. Clinoform mechanics in the Gulf of Papua, New Guinea. Continental Shelf Research 24, 2487-2510.

Weight, R.W.R., Anderson, J.B., Fernandez, R., 2011. Rapid Mud Accumulation On the Central Texas Shelf Linked To Climate Change and Sea-Level Rise. Journal of Sedimentary Research 81, 743-764.

Wheatcroft, R.A., Wiberg, P.L., Alexander, C.R., Bentley, S.J., Drake, D.E., Harris, C.K., Ogston, A.S., 2009. Post-Depositional Alteration and Preservation of Sedimentary Strata. Continental Margin Sedimentation: From Sediment Transport to Sequence Stratigraphy, 101-155.

Wright, L.D., 1971. Hydrography of South Pass, Mississippi River. Journal of the Waterways, Harbors and Coastal Engineering Division 97, 491-504.

Wright, L.D., 1977. Sediment transport and deposition at river mouths: A synthesis. Geological Society of America Bulletin 88, 857-868.

Wright, L.D., Nittrouer, C.A., 1995. Dispersal Of River Sediments In Coastal Seas - 6 Contrasting Cases. Estuaries 18, 494-508.